# UNIVERSIDAD REGIONAL AMAZÓNICA IKIAM

FACULTAD DE CIENCIAS DE LA VIDA

CARRERA DE INGENIERÍA EN BIOTECNOLOGÍA

# Understanding the behavior of *Listeria monocytogenes* within RAW264.7 macrophages, exposed the three stimulant treatments: A quantitative approach

Proyecto de investigación previo a la obtención del Título de:

**INGENIERA EN BIOTECNOLOGÍA**

**AUTOR:** MARÍA FERNANDA MINANGO CANGO

**Napo – Ecuador**

**2024**

# UNIVERSIDAD REGIONAL AMAZÓNICA IKIAM

FACULTAD DE CIENCIAS DE LA VIDA

CARRERA DE INGENIERÍA EN BIOTECNOLOGÍA

# Understanding the behavior of *Listeria monocytogenes* within RAW264.7 macrophages, exposed the three stimulant treatments: A quantitative approach

Proyecto de investigación previo a la obtención del Título de:

**INGENIERA EN BIOTECNOLOGÍA**

**AUTOR:** MARÍA FERNANDA MINANGO CANGO

**TUTOR:** MSc. MARCO ANDRÉS VITERI YÁNEZ

**COTUTOR:** MSc. MOISÉS RUBÉN GUALAPURO GUALAPURO

**Napo – Ecuador**

**2024**

**DECLARACIÓN DE DERECHO DE AUTOR, AUTENTICIDAD Y RESPONSABILIDAD**

Yo, MARÍA FERNANDA MINANGO CANGO, con documento de identidad N° 1722335161, declaró que los resultados obtenidos en la investigación que presento en este documento final, previo a la obtención del título de Ingeniería en Biotecnología, son absolutamente inéditos, originales, auténticos y personales.

En virtud de lo cual, el contenido, criterios, opiniones, resultados, análisis, interpretaciones, conclusiones, recomendaciones y todos los demás aspectos vertidos en la presente investigación son de mi autoría y de mi absoluta responsabilidad.

Tena, 5 de marzo de 2024

María Fernanda Minango Cango

1722335161

**AUTORIZACIÓN DE PUBLICACIÓN EN EL REPOSITORIO INSTITUCIONAL**

Yo, MARÍA FERNANDA MINANGO CANGO con documento de identidad 1722335161, en calidad de autor y titular de los derechos morales y patrimoniales del trabajo de titulación: “Understanding the behavior of *Listeria monocytogenes* within RAW264.7 macrophages, exposed the three stimulant treatments: A quantitative approach” de conformidad con el Art. 114 del CÓDIGO ÓRGANICO DE LA ECONOMÍA SOCIAL DE LOS CONOCIMIENTOS, CREATIVIDAD E INNOVACIÓN, reconozco a favor de la Universidad Regional Amazónica Ikiam una licencia gratuita, intransferible y no exclusiva para el uso no comercial de la obra, con fines estrictamente académicos.

Así mismo autorizo a la Universidad Regional Amazónica Ikiam para que realice la publicación de este trabajo de titulación en el Repositorio Institucional de conformidad a lo dispuesto en el Art. 144 de la Ley Orgánica de Educación superior.

Tena, 5 de marzo de 2024

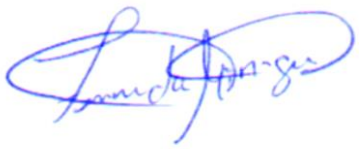

María Fernanda Minango Cango
1722335161

**CERTIFICADO DE DIRECCIÓN DE TRABAJO DE INTEGRACIÓN CURRICULAR**

Certifico que el Trabajo de Integración Curricular Titulado: Understanding the behavior of *Listeria monocytogenes* within RAW264.7 macrophages, exposed the three stimulant treatments: A quantitative approach, en la modalidad: artículo, fue realizado por: María Fernanda Minango Cango, bajo mi dirección.

El mismo ha sido revisado en su totalidad y analizado por la herramienta de verificación de similitud de contenido; por lo tanto, cumple con los requisitos teóricos, científicos, técnicos, metodológicos y legales establecidos por la Universidad Regional Amazónica Ikiam, para su entrega y defensa.

Tena, 5 de marzo de 2024

Firmado electrónicamente por:
MARCO ANDRES VITERI YANEZ

Marco Andrés Viteri Yanez

1718163759

MOISES RUBEN GUALAPURO GUALAPURO

Digitally signed by MOISES RUBEN GUALAPURO GUALAPURO
Date: 2024.03.05 14:33:49 -06'00'

Moisés Rubén Gualapuro Gualapuro

1003124284

## DEDICATORIA

Mis papás David y María, ya que, en este momento especial de mi vida quiero dar a conocer mi profunda gratitud, por el apoyo incondicional que me han brindado a lo largo de mi vida. Pues cada logro alcanzado mis padres han sido los principales impulsores siempre creyendo en mí, incluso cuando yo dudaba de mí misma. Gracias por ser mi inspiración para ser mejor persona cada día.

Mis hermanas Ana Paula y Brenda, quienes han sido mi sol en días oscuros, mis mejores amigas y confidentes. Gracias por su comprensión y paciencia en mis momentos de frustración en mi vida académica y personal, gracias por recordarme que nunca estoy sola.

Mi familia por su apoyo en cada pequeño paso que he dado a lo largo de mi vida, por cuidarme, por enseñarme, por corregirme, por brindarme todo su amor y por confiar en mí.

Mis amigos Ricardo, Joshué, Javier M., Sebastian, Javier L., Gabriel, Alexander, Mishelle, Emily, Paulina, Ana Cristina quienes he conocido a lo largo de la carrera, con quienes he pasado deberes, noches de desvelo, buenas y malas notas, buenas y malas exposiciones, fines de semana de aventuras. Con cada momento siempre fortaleciendo nuestra amistad y enriqueciendo nuestros recuerdos. Gracias por ser parte de este viaje.

A mi pequeño Mordú por alegrarme los días, por ser mi fortaleza el último año, por ser mi motivación a terminar mi carrera.

Con todo mi amor y gratitud.

## AGRADECIMIENTOS

Quiero brindar mi profundo agradecimiento a la Universidad Regional Amazónica Ikiam por haberme formado académicamente y brindarme la oportunidad de ser parte de esta prestigiosa institución y a los docentes que han sabido transmitir el conocimiento de manera excepcional.

Al Lab of Immunology, Immunity for Infection and Respiratory Medicine University of Manchester, United Kingdom, por proporcionarme los datos necesarios para desarrollar esta investigación.

A la Facultad de Ciencias de la Vida, en especial a mis tutores MSc. Marcos y MSc. Moisés por haber sido mi guía durante este proceso, por la pacienciencia que han tenido para instruirme en el tema y por su tiempo dedicación al seguimiento de mi trabajo.

Agradezco principalmente a mis padres David y María y mi hermana Paula, por estar presentes en cada etapa durante mi formación tanto académica como personal, por transmitirme sus valores y ayudarme a ser mejor persona día con día.

A mis amigos por toda la ayuda brindada en cada momento bueno o malo, por ser mi segunda familia en Tena, por el apoyo incondicional que me han dado y por su paciencia por que cada uno me ha dejado una enseñanza diferente

A William por ser una guía, por la paciencia y tiempo dedicado a enseñarme

Gracias a todos por formar parte de este camino

**TABLE OF CONTENT**

**INDEX OF TABLES**

**INDEX OF FIGURES**

**RESUMEN**

El estudio presentó un análisis del crecimiento de *Listeria monocytogenes* y desarrolló modelos predictivos para su comportamiento. Se enfocó en el impacto de tratamientos como Interferón alfa (IFN-α) y el Regulador de Proteínas de Listeria Virulencia A en el crecimiento de *L. monocytogene*s. Se detallaron los métodos de adquisición de datos, conteo, monitoreo automático, preprocesamiento de datos y construcción de algoritmos de análisis de imágenes. Se emplearon cuatro modelos matemáticos (Gompertz, Baranyi, Logistic y Richards) para ajustar las curvas de crecimiento de *L. monocytogene*s y comparar los parámetros. Se encontró que el modelo de Gompertz proporcionó el mejor ajuste para el crecimiento bajo tratamiento con interferón alfa. Los resultados indicaron una reducción significativa del crecimiento bacteriano con el tratamiento de interferón alfa, mientras que el tratamiento con PrfA promovió el crecimiento. El tratamiento de control permitió el crecimiento bacteriano sin restricciones. En conclusión, el estudio proporcionó información valiosa sobre la dinámica del crecimiento de *L. monocytogene*s y el impacto de los tratamientos en su proliferación. Se demostró la efectividad del interferón alfa para reducir el crecimiento bacteriano y se identificó el modelo de Gompertz como el más adecuado para predecir el crecimiento bajo tratamiento con interferón alfa. Estos hallazgos son cruciales para mejorar las evaluaciones de seguridad alimentaria y predecir la vida útil de los productos alimenticios.

**Palabras clave**
*Listeria monocytogenes,* modelado matemático, crecimiento bacteriano, interferon alpha, PrfA.

**ABSTRACT**

The study presented an analysis of the growth of *Listeria monocytogenes* and developed predictive models for its behavior. It focused on the impact of treatments such as Interferon alpha (IFN-α) and Listeria Protein Regulator Virulence A on the growth of *L. monocytogenes*. The methods of data acquisition, counting, automatic monitoring, data preprocessing, and construction of image analysis algorithms were detailed. Four mathematical models (Gompertz, Baranyi, Logistic and Richards) were used to fit the growth curves of *L. monocytogenes* and compare the parameters. It was found that the Gompertz model provided the best fit for growth under interferon alfa treatment. The results indicated a significant reduction in bacterial growth with interferon alpha treatment, while PrfA treatment promoted growth. The control treatment allowed unrestricted bacterial growth. In conclusion, the study provided valuable information on the growth dynamics of *L. monocytogenes* and the impact of treatments on its proliferation. The effectiveness of interferon alfa in reducing bacterial growth was demonstrated and the Gompertz model was identified as the most appropriate to predict growth under treatment with interferon alfa. These findings are crucial for improving food safety assessments and predicting the shelf life of food products.

**Keywords**
*Listeria monocytogenes,* mathematical modeling, bacterial growth, interferon alpha, PrfA.

## BACKGROUND

Parasitic diseases result from various infectious agents, spanning bacteria protozoa to parasitic worms. Many pathogens undergo intricate life cycles, necessitate vector transmission, or involve intermediate hosts. While only a select few of these parasites can be highly fatal, many induce chronic infections that often lead to severe illnesses, imposing a significant global burden on human and animal health (Nag & Kalita, 2022). Beyond the imperative of addressing health challenges, there is also a genuine curiosity to unravel the unique biology of these remarkable pathogens. Intracellular bacteria can thrive and replicate within single-celled phagocytes, as they can reproduce independently of the host cell (Kaufmann, 1993). Single-cell phagocytes serve as potent effector cells capable of engulfing and eliminating numerous bacterial invaders (Nag & Kalita, 2022). However, failure in this defense mechanism can result in these bacteria causing various diseases that impact both human and animal health. These bacteria invade and establish colonies within the intracellular niche of eukaryotic cells (Flannagan et al., 2009). Invasion refers to penetrating host cells from tissues through a complex array of molecules commonly known as "invasins". At this stage, these invasins may take the form of secreted proteins on the bacterial surface that target specific host cell molecules known as receptors. These invasins can generate biologically active molecules, such as toxins, which cause tissue damage locally or at a distance (Khan et al., 2016). However, the attachment of pathogens to mucosal surfaces represents only the initial phase of tissue invasion (Maria Fátima Horta et al., 2020).

The initial step in cellular invasion involves breaching the body's cell membrane, and many intracellular pathogens utilize common phagocytic entry mechanisms to gain access (Maria Fátima Horta et al., 2020). The host cell surrounds these pathogens with membrane vesicles once they enter the cell. The ability of intracellular pathogens to escape from these vesicles determines the host cell type they engage with. Consequently, some pathogens can invade various cell types, while others exhibit limited invasiveness. In this process, researchers have identified rece ptors specific to different invading pathogens. Both primary and opportunistic pathogens possess virulence determinants or invasive factors contributing to disease development. Numerous bacteria exhibit multiple virulence determinants, each playing a distinct role in various stages of the disease process (Sura A. Abdulateef et al., 2023). Moreover, not all strains within a particular bacterial species display equal levels of pathogenicity.

Modifiers of toxicity encompass factors such as the availability of nutrients, oxygen, appropriate temperature, or other growth necessities (Brian Henderson & Andrew Martin, 2011). Among the diseases caused by such bacteria are tuberculosis, typhoid fever, listeriosis, chlamydiosis, brucellosis, rickettsiosis, Q fever, legionellosis, and listeriosis. Bacteria from genera such as *Rickettsia spp, Chlamydia spp, Coxiella spp, and Listeria spp* are attributed to these pathologies (Allerberger & Wagner, 2010).

*Listeria monocytogenes (L. monocytogenes)* is a gram-positive bacillus bacteria with facultative anaerobic characteristics, allowing it to thrive in oxygen-rich and oxygen-deprived environments (Southwick & Purich, 1996). Within the host, it demonstrates intracellular behavior, multiplying and surviving to gain a competitive advantage. This bacterium resists cool temperatures, maintaining its reproduction ability at 2 to 4 degrees Celsius (Iharilalao Dubail et al., 2000). Characterized by actin rockets, *L. monocytogenes* displays explosive activity, polymerizing actin filaments that enable it to move within the host cell and promoting increased activity in actin filament polymerization. (Theriot et al., 1992). The distinctive "tumbling motility," observed under a microscope, involves somersault-like movements. The catalase-positive nature of *L. monocytogenes* allows it to transform hydrogen peroxide into water and oxygen, aiding in its identification. It possesses beta-hemolytic properties and destroys red blood cells, detectable in blood agar through the illuminated edge of the bacterial growth area. Notably, *L. monocytogenes* is the sole gram-positive bacterium with a gram-negative structure, although lacking endotoxin characteristics (Iharilalao Dubail et al., 2000). Upon entering the digestive tract, *L. monocytogenes* encounters macrophages and epithelial cells. It enters macrophages through phagocytosis and epithelial cells through endocytosis, mediated by specific receptors interacting with ligandins on the bacterium. Facilitating phagocytosis, internaline A and B assist in entering *L. monocytogenes* into macrophages. Within the phagolysosome, the bacterium smoothens and breaks it down using listeriolysin O and phospholipase C (Cossart et al., 2003). Once free in the cytoplasm, the bacterium multiplies, aided by the surface protein ActA, which activates the synthesis of actin filaments, promoting mobility within the macrophage (Pizarro-Cerdá et al., 2012). Actin rockets are formed, along with "tumbling motility," as the bacterium presses from within, making contact with other macrophages and entering their cytoplasm. This process continues through the lysis of new phagolysosomes by listeriolysin O and phospholipase C. Beyond the small intestine, this activity spreads through lymphoid tissue to organs such as the liver or spleen. The bacterium's ability to breach the blood-brain and placental barriers poses risks, leading to fetal complications

in pregnant women (Pizarro-Cerdá et al., 2012).

The problem with *Listeria monocytogenes* goes beyond its ability to fool the immune system and establish persistent infections (Espinosa-Mata et al., 2022). One of the concerning characteristics of *Listeria monocytogenes* is its ability to form biofilms on (Reguera, 1995) the surfaces of equipment and cooking utensils in food facilities. Biofilms provide a protective environment that makes the bacterium highly resistant to conventional cleaning and disinfection procedures, making it difficult to eradicate and in food production (Lasa et al., 2005). In addition, the ability of *Listeria monocytogenes* to grow at refrigeration temperatures makes it a particular hazard in ready-to-eat products that do not require further cooking, such as salads, deli meats, and dairy products (Orsi et al., 2011). This means that consumers may be exposed to the bacteria without knowing it, increasing the risk of serious illness, especially in vulnerable populations such as pregnant women, newborns, the elderly, and those with compromised immune systems (Espinosa-Mata et al., 2022). The detection and control of *Listeria monocytogenes* in the food industry are ongoing challenges. Although strict quality control programs and preventive measures, such as regular monitoring of facilities and products, as well as training of personnel in proper hygienic practices, are implemented, the persistence of the bacteria remains a significant concern (Reguera, 1995). *Listeria monocytogenes* has been found in foods such as soft cheeses, yogurt, and processed foods in general, in addition to the bacterium on the surfaces of factories dedicated to the food area, increasing the risk of cross-contamination. Even existing control analysis within Ecuadorian establishments, in a study conducted in 2018 it has been reported that in samples collected in 18 of the 24 provinces, 14.23% represents *L. monocytogenes*, having prevalence in provinces such as Carchi and Pichincha (Espinosa-Mata et al., 2022).

Considering the complexity of the interaction between *Listeria monocytogenes* and the host immune system, the need to further investigate the dynamics of *L. monocytogenes* bacterial populations within macrophages is evident. This approach is crucial not only to understand the pathogenesis of infections by this bacterium but also to develop more effective therapeutic and control strategies. Unraveling how *L. monocytogenes* modulates the host immune response and persists within macrophages is essential, as this provides valuable information that can guide the design of interventions to prevent and treat *L. monocytogenes* infections more effectively. However, much remains to be learned about the behavior of the *L. monocytogenes* bacterium in macrophages and how

it responds to different treatments. Specifically, it is necessary to understand the quantitative behavior of this bacterium when faced with different treatments such as interferon alpha, interferon alpha 2X, and PrfA in the macrophages of the RAW264.7 cell line.

Interferon alpha (IFN-α) is a naturally occurring protein produced by the immune system, playing a crucial role in the body's defense against microbes. In the specific context of combating *L. monocytogenes*, IFN-α exhibits several key characteristics. Firstly, it demonstrates antiviral and antimicrobial action by impeding the proliferation of bacteria, thereby limiting the spread of *L. monocytogenes* within the body (Ohya et al., 2003). Secondly, IFN-α is instrumental in stimulating the immune response. It aids in the maturation and activation of essential immune cells, including dendritic cells, macrophages, and natural killer (NK) cells. Additionally, it induces the production of proinflammatory cytokines, which recruit and activate various components of the immune system, enhancing the overall defense against the pathogen (Aubry et al., 2012). Furthermore, IFN-α displays cytotoxic activity, exerting potential effects against cells infected with *L. monocytogenes* (Ohya et al., 2003). This includes the ability to induce apoptosis, or programmed cell death, in infected cells, contributing to eliminating the pathogen and restricting its dissemination. Moreover, IFN-α enhances antigen presentation, improving the ability of cells to present pathogenic fragments to the immune system. This augmentation facilitates a more robust and effective immune response against *L. monocytogenes* (Aubry et al., 2012). It is important to note that while IFN-α is commonly used in treating specific viral infections and immune-related conditions, its application in combating *Listeria monocytogenes* infection may depend on various factors, including the severity of the disease and the unique response of individual patients (George et al., 2012).

A treatment approach akin to Protein Regulator of *Listeria* Virulence A (PrfA) involves targeting a pivotal transcription factor in *L. monocytogenes,* the causative agent of listeriosis (Torres et al., 2005). PrfA assumes a critical role in the virulence of *L. monocytogenes* by orchestrating the expression of genes crucial for intracellular invasion and survival (de las Heras et al., 2011; Miner et al., 2007). The distinctive characteristics of PrfA that contribute to combating *L. monocytogenes.* It is responsible for regulating virulence gene expression, as it controls the expression of numerous virulence genes in *L. monocytogenes* (Torres et al., 2005), influencing processes such as host cell adhesion and entry, phagosome escape, intracellular replication, and

resistance to host immune response. By up-regulating these genes, PrfA increases the ability of *L. monocytogenes* to infect and persist within host cells (Miner et al., 2007). Activation by Environmental Stimuli, notably temperature and pH. Activation occurs in conditions mimicking the human host, where body temperature and neutral pH stimulate PrfA function. This activation is crucial for *L. monocytogenes* to adopt its active and virulent form, evading host defenses and instigating infection (Miner et al., 2007). Autonomous Regulation and Self-Amplification feature means that once started by specific conditions, PrfA can augment its activity, sustaining virulence gene expression continuously (de las Heras et al., 2011). This self-amplification is pivotal for the persistence and dissemination of *L. monocytogenes* within the host. Interaction with other virulence factors within *L. monocytogenes*, orchestrating gene expression and modulating the response of the pathogen to various environmental conditions (Jung et al., 2002); this includes interactions with proteins such as ActA, which influence the intracellular motility of *L. monocytogenes*, and the formation of actin protrusions that facilitate cell-to-cell spread. The exploration of PrfA and its role in the virulence of *L. monocytogenes* has been instrumental in comprehending the infection mechanisms of this bacterium. Additionally, it has furnished crucial insights for developing therapeutic and preventive strategies against listeriosis (Brinkmann et al., 2004). *Listeria monocytogenes* is a valuable model pathogen for research due to its reproducible infection and ability to easily account for bacteria-host interactions despite their complexity. The host response to *L. monocytogenes* involves two primary types of immune responses: innate and adaptive immune responses (Jung et al., 2002).

Broadly speaking, the RAW264.7 cell line is a mouse-derived macrophage cell line widely used in biological and medical research. It was developed from mouse peritoneal macrophage cells and has become a fundamental cell model for studying various biological processes, including immunology, inflammation, cancer biology, and immune response (InvivoGen, 2016). RAW264.7 cells are immune cells of the monocyte/macrophage lineage that can adhere to cell culture surfaces and phagocytize foreign particles, such as bacteria and cellular debris. These cells are characterized by their ability to proliferate in culture and maintain the functional characteristics of primary macrophages (Wei et al., 2022). Because of their ease of culture, genetic stability, and ability to reproduce responses similar to primary macrophages under certain conditions, RAW264.7 cells are widely used in in vitro studies to investigate a variety of biological processes, therapeutic compounds, anti-inflammatory agents and to test the efficacy of potential drugs (Zheng et al., 2019).

Fluorescence microscopy employs the ability of certain molecules to absorb light at specific wavelengths and then emit light at longer wavelengths. In the case of RAW264.7 with Lm-GFP, this technique makes it possible to visualize the interaction between the RAW264.7 cell line and Lm-GFP (*Listeria monocytogenes* green fluorescent protein). This approach allows us to observe how RAW264.7 cells internalize Lm-GFP and study the infection dynamics (Elisia et al., 2018). Although precise details on using RAW264.7 with Lm-GFP are not available in the search results, it is suggested to consult specialized sources in microbiology, immunology, or cell biology for additional information or specific details on this application. The importance of this technique lies in its ability to visualize cellular processes in real-time and in detail, which provides valuable information on the dynamics of infection and immune response. In addition, fluorescence microscopy is a non-invasive technique that does not require fixation or staining of the cells, allowing the study of cellular processes under conditions closer to normal physiological conditions (Elisia et al., 2018; Garzón, 2011).

This research aims to obtain, through a quantitative approach derived from modeling bacterial growth with fluorescence microscopy imaging data, the behavior of the *Listeria monocytogenes* bacterial population exposed to three specific study treatments in RAW264.7 macrophages. For this purpose, segmentation and tracking algorithms will be applied to fluorescence microscopy images of live cells of RAW264.7 macrophages infected with *Listeria monocytogenes* to perform modeling of bacterial growth in four different mathematical models which are Baranyi, Gompertz, Logistic, Richards. Subsequently, the results of the bacterial growth modeling will be analyzed using the best-fitting model to identify patterns or trends in the behavior of the bacterial population of *Listeria monocytogenes* in response to treatment with interferon-alpha, interferon alpha 2X, and PrfA. These objectives aim to gain a deeper understanding of the interaction dynamics between *Listeria monocytogenes* and macrophages and to assess the impact of different treatments on the growth and behavior of this intracellular bacterium.

## METHODS

This is a brief description of the methodology used in this research.

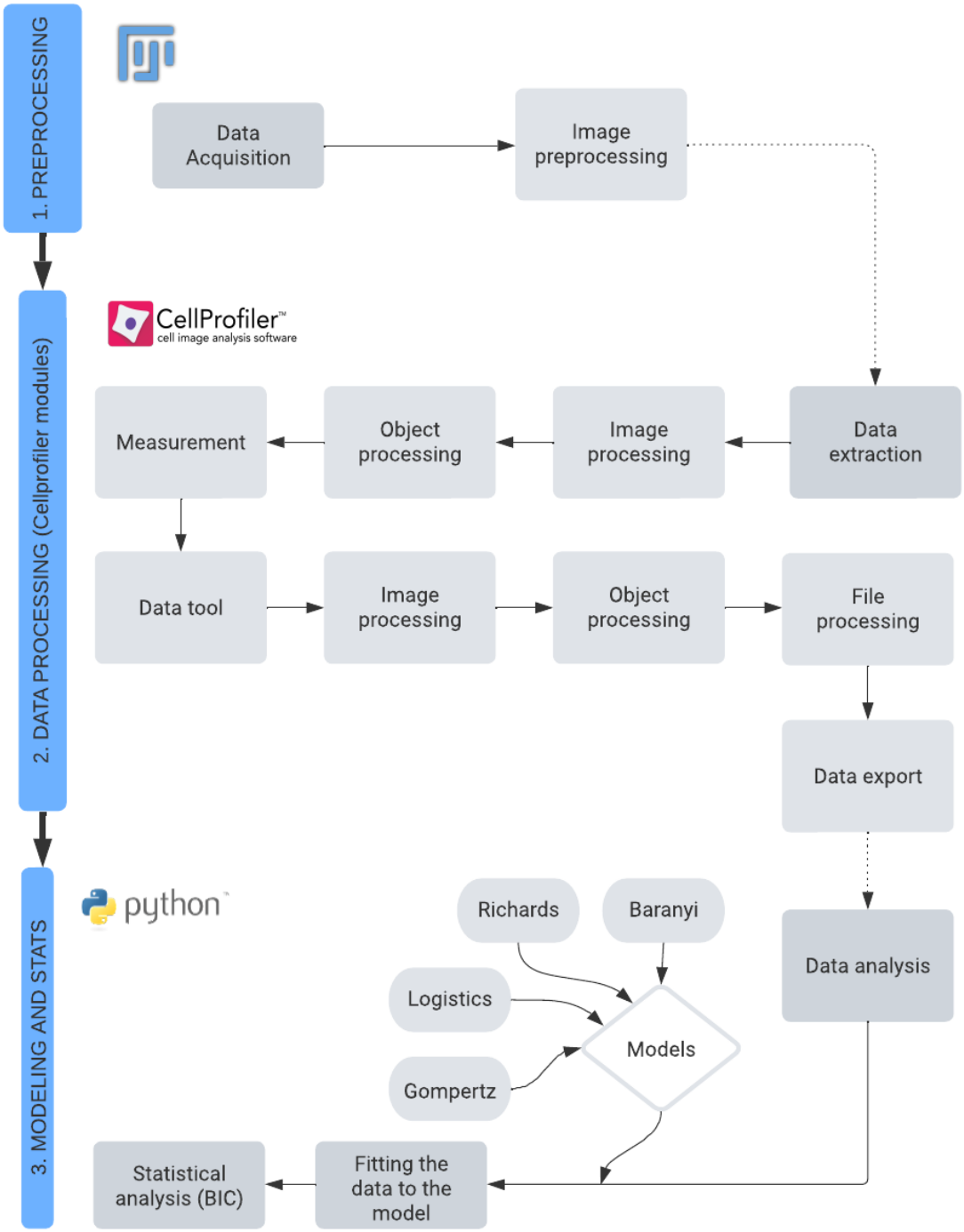


**Figure 1:** Methodology flowchart
**Made by:** Minango María, 2024.

## Data Acquisition

Experiments on macrophage infection by *L. monocytogenes* were made at the Lab of Immunology, Immunity for Infection and Respiratory Medicine at University of Manchester, United Kingdom. Live cell fluorescent microscopy images were acquired with an ACQUIFER Next Generation Imaging and High Content Screening [Germany] fluorescence microscope in ".mov" format. Provided image datasets were 27 files for the first test and 36 files for each of the other 3 test. In each file, there were at least 100 frames for each treatment, and each frame was captured within 5 minutes

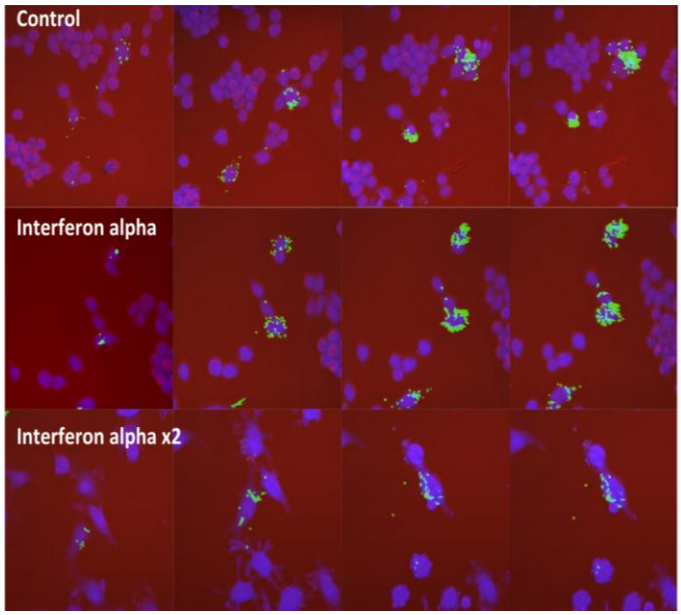


**Figure 2:** Growth of *Listeria monocytogenes* in the first test, of which there is only data from the control trial, which does not have a controller of the bacterial population growth, interferon alpha, and interferon alpha with the doubled dose. In the first box of the microscope.
**Taken by:** Moran Josephine, 2020.
**Processed by:** Minango María, 2023.

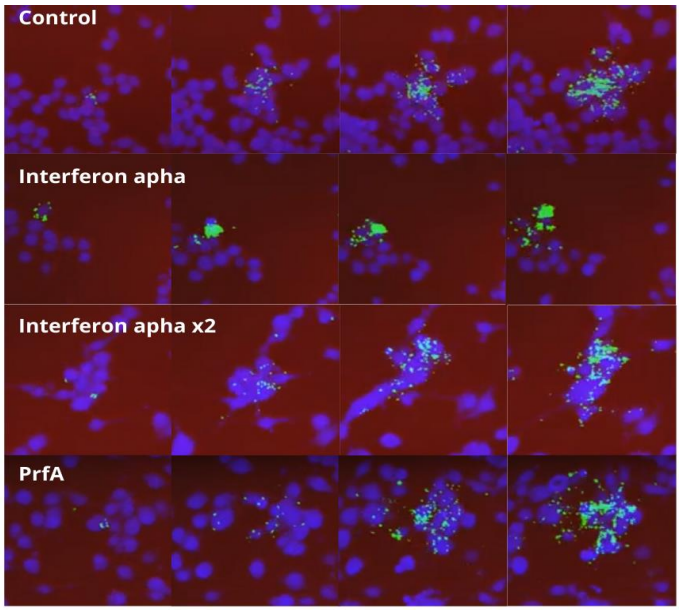


**Figure 3:** Growth of *Listeria monocytogenes* in second test, control which does not carry any controller of the bacterial population growth, Interferon alpha, interferon alpha with the doubled dose and PrfA as treatments respectively. In the first box of the microscope.
**Taken by:** Moran Josephine, 2020.
**Processed by:** Minango María, 2023.

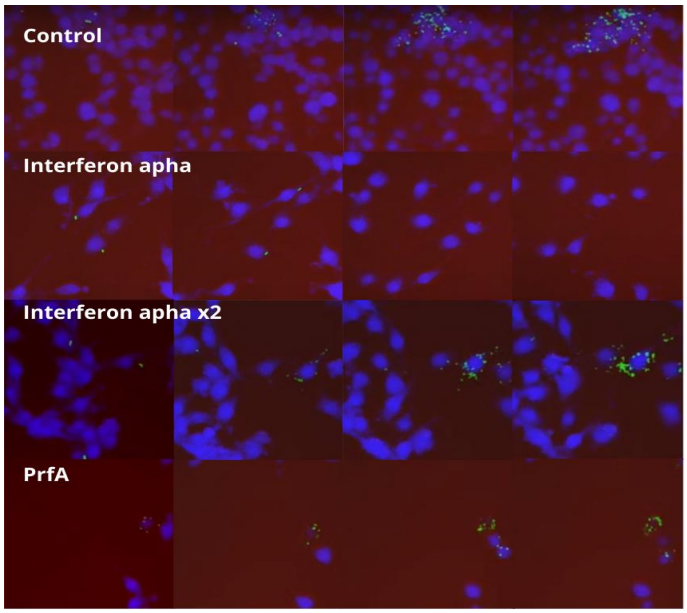


**Figure 4:** Growth of *Listeria monocytogenes* in third test, control which does not carry any controller of the bacterial population growth, Interferon alpha, interferon alpha with the doubled dose and PrfA as treatments respectively. In the first box of the microscope.
**Taken by:** Moran Josephine, 2020.
**Processed by:** Minango María, 2023.

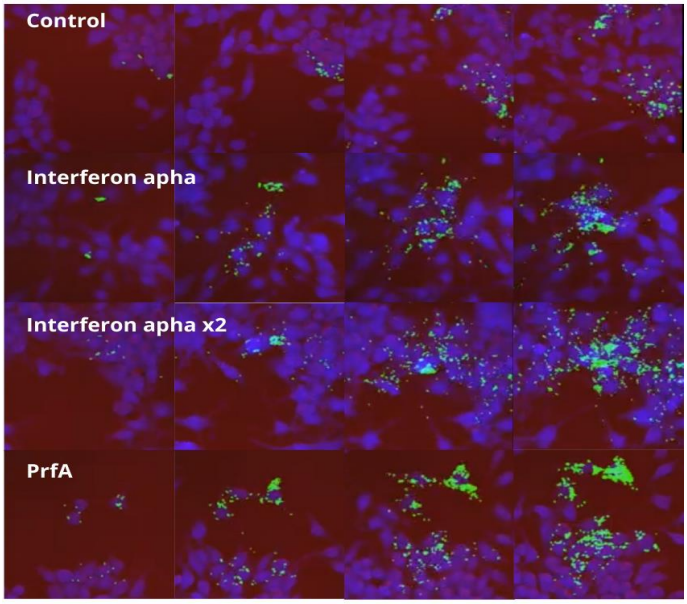


**Figure 5:** Growth of *Listeria monocytogenes* in the fourth test, control which does not carry any controller of the bacterial population growth, Interferon alpha, interferon alpha with the doubled dose and PrfA as treatments, respectively. In the first box of the microscope.
**Taken by:** Moran Josephine, 2020.
**Processed by:** Minango María, 2023.

### Counting and automatic monitoring

### Data preprocessing with ImageJ

Fiji is an image processing package—a "batteries-included" distribution of ImageJ, bundling many plugins that facilitate scientific image analysis (Schindelin, 2012). To solve everyday microscopy image analysis tasks. As an open-source Java-based software developed at the National Institutes of Health, it facilitates project development. It can display, edit, analyze, process, save, and print 8-bit, 16-bit, and 32-bit images and supports major image formats such as TIFF, GIF, JPEG, BMP, DICOM, FITS, and raw. ImageJ's main features include area and pixel value calculations, distance and angle measurements, density histograms, and line profile plots. It also supports standard image processing functions such as contrast manipulation, sharpening, smoothing, edge detection, and median filtering (Sánchez, 2014).

Using the image program. The data was separated into three bands. The green band corresponds to bacteria, stored in folder 1 with a labeling protocol. The blue band corresponds to macrophages accumulated in folder 2 with the labeling protocol. The

images processed by ImageJ are saved in tiff stacks in a sequential format (Bankhead, 2014).

**Data processing with Cellprofiler**

Microscopy in research has evolved with increasing automation, allowing detailed images to be captured of samples treated with various compounds or genetic perturbations, even in 3D or time series (Stirling et al., 2021). Analysis of these images requires specialized software, but proprietary packages can be expensive and limited in flexibility. Therefore, open source tools have gained popularity, offering automated and quantitative analysis (*NIH Image to ImageJ: 25 años de análisis de imágenes | Métodos de la naturaleza*, s/f). In 2005, CellProfiler, an open source image analysis program that revolutionized the ability of users without specific training to automate image analysis using modular processing pipelines, was introduced (Wiesmann et al., 2015). This tool has gained wide acceptance, being referenced more than 2000 times a year. CellProfiler offers integrated modules with various algorithms for image analysis, and its flexibility is further extended by community-developed add-ons. In independent comparisons, CellProfiler has stood out with high ratings in usability and functionality (McQuin et al., 2018).

**Data extraction module**

The image field was loaded in folders in the Cell Profiler program for extraction. A regular expression is constructed in the metadata to differentiate images, bacteria, and macrophages. The photos were labeled by name and typed by the generated typologies in this section.

**Image processing module**

First, distinguish the type of image to be presented. For the illumination function, the split option was applied. Then, the edges were enhanced with the Sobel function, considering their direction. It was smooth the images by polynomial adjustment. It were used a thresholding strategy by calculating the threshold value based on pixels through minimum cross-entropy.

**Object processing module**

Two parameters were distinguished within the images to evaluate bacteria and macrophages. It identified bacteria as the primary object. To be identified, a range between 6 and 20 pixels was set. In macrophages, it was considered the nucleus of the cells as the primary object. It was selected at a range of 20 to 60 pixels for identification. It discarded objects outside the fixed scope for direct things but included objects touching the edge of the image. It was identified as a secondary object in macrophages as the cytoplasm using propagation. The strategy for threshold identification was adaptive, involving three classes: foreground, background, and intermediate intensity. Pixels falling into the medium-intensity category were reassigned to the foreground. For this purpose, the threshold smoothing scale was selected from 1.3 to 1.8, and a correction factor value close to 0.8 was applied. An adaptive window size of 60 was chosen. The regularization factor was set at 0.05. Subsequently, the holes of the selected objects were filled, and secondary objects touching the edge of the image were not discarded. The defined region was masked using the primary identification objects of bacteria. Objects that are partially masked and overlapping were removed based on the overlap. To track the objects, the minimum distance and the distance from the centroid was calculated.

**Measurement module**

The overlap of the objects was measured by selecting the image to be used as a basis for calculating the amount of overlap.

**Data tool module**

The object measurements were displayed by text input with a size of twelve points and three decimal places. Afterwards, the output image is named, and the element is saved in image type.

**File processing module**

The data obtained was exported to a spreadsheet with specifications. A column delimiter and a prefix for the file name were selected. On the other hand, the images were saved in tiff format.

**Data export module**

The measurement variables of the images and objects are selected, and then the output files are defined. The ".csv" outputs were selected. It was necessary to export it in this format for subsequent analysis in the Python program, in which mathematical models were applied to construct the image analysis algorithm.

**Detailed explanation of Model parameters are in the model fitting section**

The ability to count and monitor automatically enables efficient and accurate data collection, facilitating the understanding of complex phenomena and fundamental decision-making. In the field of microbiology, the ability to automatically count and monitor bacteria is essential to understand their behavior and response to different environmental conditions and treatments. In this context, mathematical models such as Gompertz, Baranyi, Logistic and Richards play a fundamental role in providing tools to describe and predict bacterial population growth (Gonzalez Cuello et al., 2022; Tjørve & Tjørve, 2017; Ulloa Ibarra et al., 2017; Ulloa Ibarra & Rodriguez Carrillo, 2010).

**Gompertz Model**

The Gompertz function is a valuable tool in the mathematical modeling of growth processes in various disciplines, such as biology and economics. By exploring the modified Gompertz function, It could break down the meaning of its key parameters and understand how they influence the shape of the growth curve [30].

$$f(x) = A \cdot e^{-u \cdot e - q \cdot x}$$

**Equation 1:** Gompertz Model

A: Asymptotic upper limit represents the maximum value the function will reach as the independent variable "x". This value encapsulates the full magnitude of growth over time.

u: Affects the initial growth rate. Higher values of u indicate a faster initial growth rate. In other words, u affects the slope of the growth curve at the beginning of the process.

q: Affects the rate of exponential decay, related to the speed of exponential decay.

Higher values of q suggest a slower decline in the growth rate as the independent variable increases. This parameter models how growth slows over time.

x: Independent variable represents time. The Gompertz function describes how the dependent variable y changes relative to x.

By fitting these parameters, It could adapt the Gompertz model to the specific data and phenomena they were studying. Experimenting with A, u, and q allows us to reflect the growth dynamics observed in population growth accurately.

**Baranyi Model**

This equation models the growth of a microbial population over time. The presence of exponential terms e^(u·x) indicates the dependence of growth on time, and the fraction in the denominator adjusts the growth rate as a function of the current population and the upper limit [31].

$$y = \frac{y_0 \cdot A \cdot (1 + q \cdot e^{u \cdot x})}{\frac{A - y_0 + y_0(1 + q \cdot e^{u \cdot x})}{(1 + q)}}$$

**Equation 2:** Baranyi Model

y: The dependent variable represents the microbial population at a given time.

y_0: The initial microbial population at time t = 0. It is the starting point from which growth begins.
x: is the independent variable, representing time.

A: The asymptotic upper limit of the microbial population, i.e., the maximum value that the population can reach under ideal conditions.

q: It is a parameter that affects the rate of adjustment of the growth rate. It is associated with the speed of adjustment of the growth rate as a function of time. A higher value of u implies a faster adjustment in the initial growth rate. It controls how quickly the microbial population responds to the environment and begins to grow.

u: It is a parameter that also affects the speed of growth rate adjustment. However, It influences over time in such a way that A higher value of q may indicate a slower deceleration in growth rate as the population approaches the asymptotic upper limit. It has an effect on the shape of the growth curve, especially in the deceleration phase.

By adjusting the values of the parameters A, y0, q, y, you can adapt the equation to represent different microbial growth scenarios under specific conditions. This Baranyi model provides a flexible way to model microbial population dynamics in various contexts.

**Logistics Model**

The logistic function is an essential tool in growth modeling, and the equation provided allows us to analyze its dynamics in detail [32]. Let's break down the interpretation of each parameter:

$$y = \frac{A}{1 + e^{(\frac{4u}{A})(q-x+2)}}$$

**Equation 3:** Logistics Model

A: Carrying Capacity or Asymptotic Upper Limit of the population. This value indicates the maximum population that the environment can support, serving as a ceiling for growth.

u: Factor Affecting the Slope of the logistic curve. A higher value of u may result in a steeper transition between growth phases. This parameter models the sensitivity of the population to changes in environmental conditions.

q: Horizontal shift of the logistic curve. The higher the value of q, the sooner or later the inflection in growth will occur. This parameter indicates the time at which the population reaches half of its carrying capacity. The logistic equation models the population as a function of time.

x. By manipulating the values of A, u, and q, it could adjust the specific shape of the logistic curve and adapt it to different growth scenarios, from populations that stabilize quickly to those that experience a more gradual expansion.

This logistic model provides a versatile framework for understanding and predicting growth patterns in various disciplines, allowing researchers to effectively capture the complexity of real-world growth phenomena.

**Richards Model**

The Richards function is a powerful tool in growth modeling [33]. Let's break down the interpretation of each parameter:

$$y = A(1 + v \cdot exp(1 + v)exp)(\frac{u}{A}(1 + v)(1 + \frac{1}{v})(q + x))$$

**Equation 4.** Richards Model

A: Asymptotic Upper Limit of the population, representing the maximum value the population can reach under ideal conditions. This parameter establishes the ceiling for growth.

u: Factor Affecting the Slope of the Richards curve. A higher value of u may result in a more abrupt or smoothed transition between growth phases, depending on the importance of v. This parameter models the sensitivity of the population to changes in environmental conditions.

q: Horizontal displacement of the Richards curve. The higher the q value, the sooner the inflection in growth will occur. This parameter indicates the time the population reaches the middle of its upper limit.

v: Controls the shape of the Richards Curve. Higher values of v may result in a smoother curve, while lower values may produce a steeper angle. This parameter is essential for adjusting the specific shape of the growth.

The Richards equation models the population as a function of time x. By manipulating the values of A, u, q, and v, It could tailor the shape of the Richards curve and represent a wide range of growth dynamics observed in reality.

**Fitting the data to the model**

The consolidated data from the CellProfiler program were fitted in Python using the SciPy, *lmfit, NumPy* and *Matplotlib* libraries. A function was created based on each model, of which the R2 was evaluated to verify the effectiveness of the model. A graph was obtained with the 4 treatments which are Control, Interferon alpha, interferon alpha with doubled dose, and PrfA, for each model in each test Made.

**Statistical analysis**

Select the growth rate parameters and evaluate if there are significant differences between the different treatments using Bayesian Information Criteria (BIC). This was chosen over other models because of its ability to penalize model complexity more strictly than other criteria. BIC looks for the most abstract and most straightforward model, which makes it helpful in selecting simpler models that can still explain the data effectively. When comparing several models, the model with the lowest BIC value is considered to have the best quality in the model set (Hilbe, 2017).

## RESULTS

Using software such as ImageJ, the separation of the red, green, and blue channels, corresponding to the background, bacteria, and macrophage, respectively, have been achieved. These have been used for data processing in Cellprofiler, which allowed tracking the population growth of *Listeria monocytogenes* in conjunction with the RAW264.7 macrophage.

### Construction of the image analysis algorithm

Sixteen graphs were obtained representing the 4 mathematical models chosen for the research coupled to the 4 tests.

### Baranyi Model

The analysis of bacterial growth of *Listeria monocytogenes* using the Baranyi model (**Figure 6**) has yielded promising results. The three treatments evaluated - control, interferon alpha, and interferon alpha - have shown a high ability to fit the proposed model. The coefficients of determination (R2) obtained for each treatment are significant, registering values of 0.97, 0.959 and 0.969, respectively. These results suggest that the Baranyi model can capture bacterial growth accurately and representatively under the evaluated treatments.

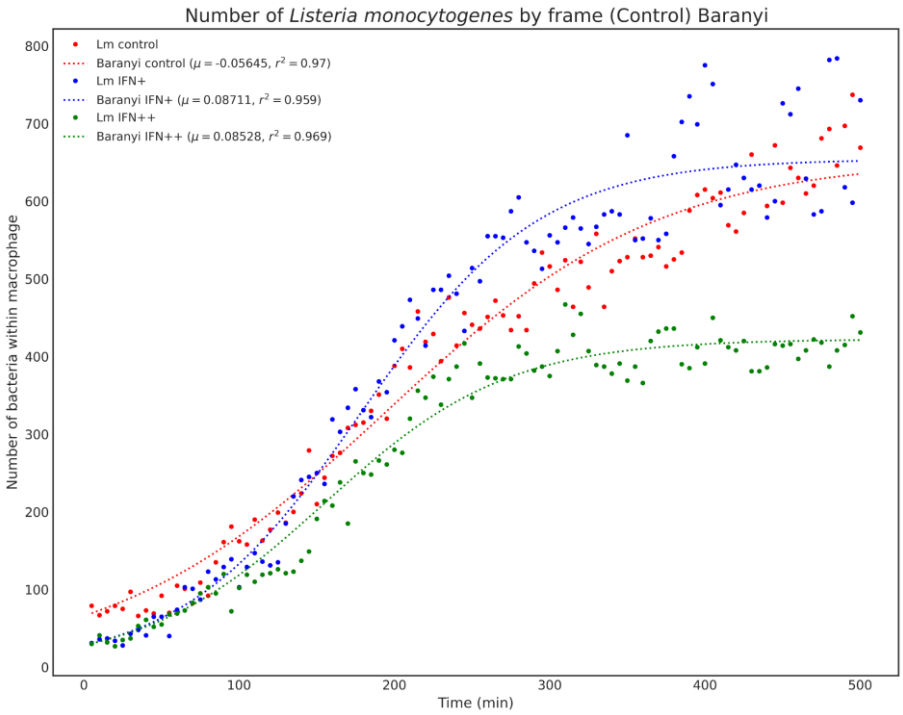


**Figure 6:** Baranyi modeling first test with control, interferon alpha, and interferon alpha with doubled dose at 500 minutes.

**Made by:** Minango María, 2023.

Four different treatments were examined: control, interferon alpha, interferon alpha and PrfA, each of which was modeled using the Baranyi approach (**Figure 7**). The coefficients of determination (R2) obtained for each treatment were 0.949, 0.973, 0.97 and 0.954, respectively, indicating an acceptable fit of the Baranyi model to the experimental data.

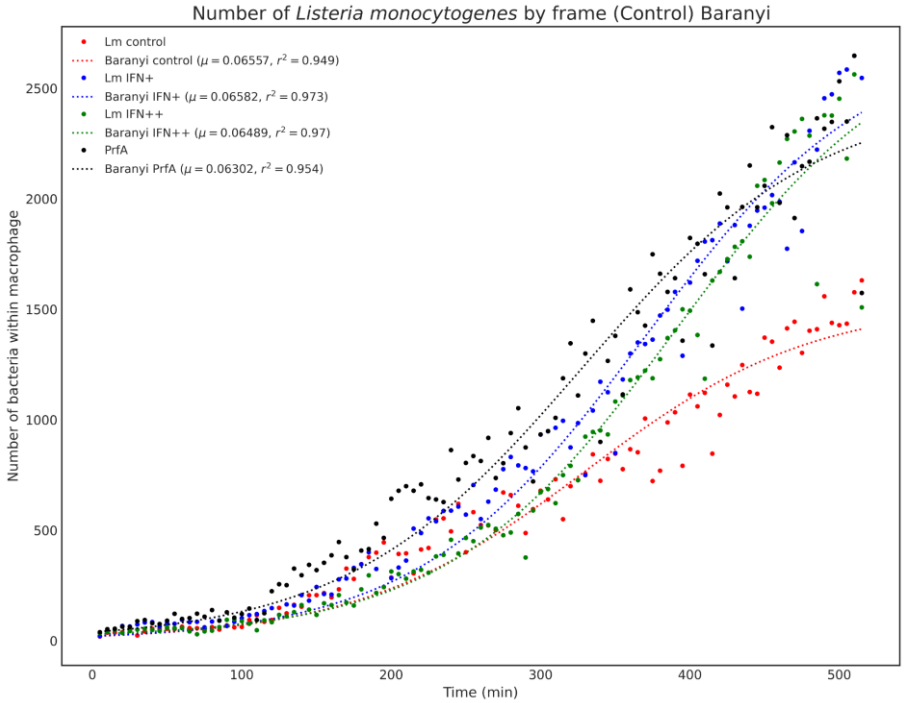


**Figure 7:** Baranyi modeling second test with control, interferon alpha, interferon alpha with doubled dose and PrfA at 500 minutes.
**Made by:** Minango María, 2023.

Four different treatments were evaluated: control, interferon alpha, interferon alpha and PrfA (**Figure 8**). Each treatment was modeled using the Baranyi growth model, with corresponding coefficients of determination (R2) of 0.962, 0.812, 0.865 and 0.785, respectively.

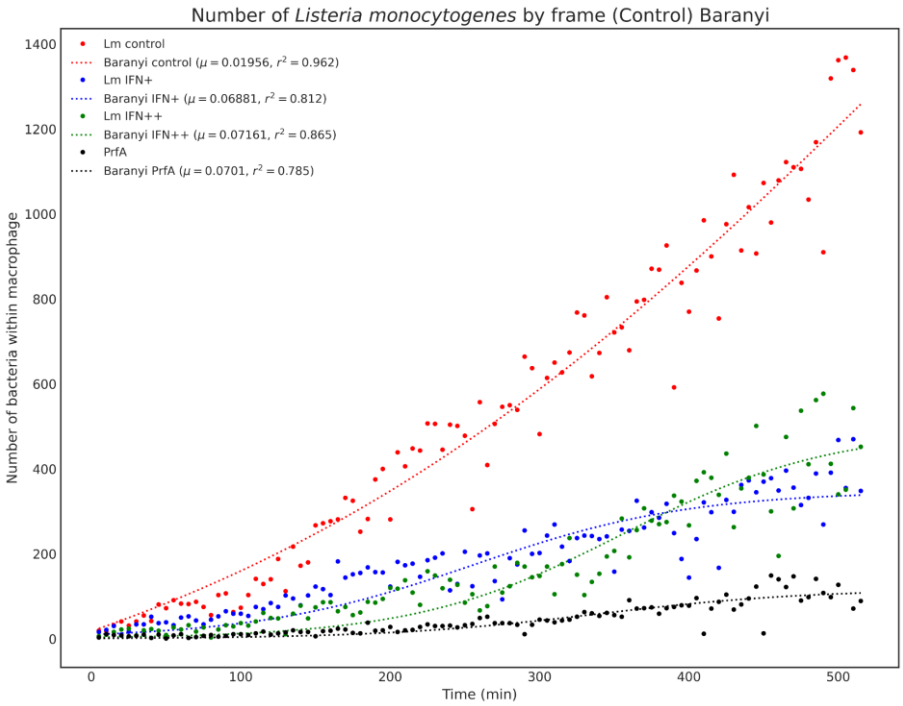


**Figure 8:** Baranyi modeling third test with control, interferon alpha, interferon alpha with doubled dose and PrfA at 500 minutes.
**Made by:** Minango María, 2023.

Four different treatments were evaluated: control, interferon alfa, interferon alfa and PrfA (**Figure 9**). Each treatment was modeled using the Baranyi approach, and the coefficients of determination (R2) obtained were 0.979, 0.956, 0.988 and 0.942, respectively.

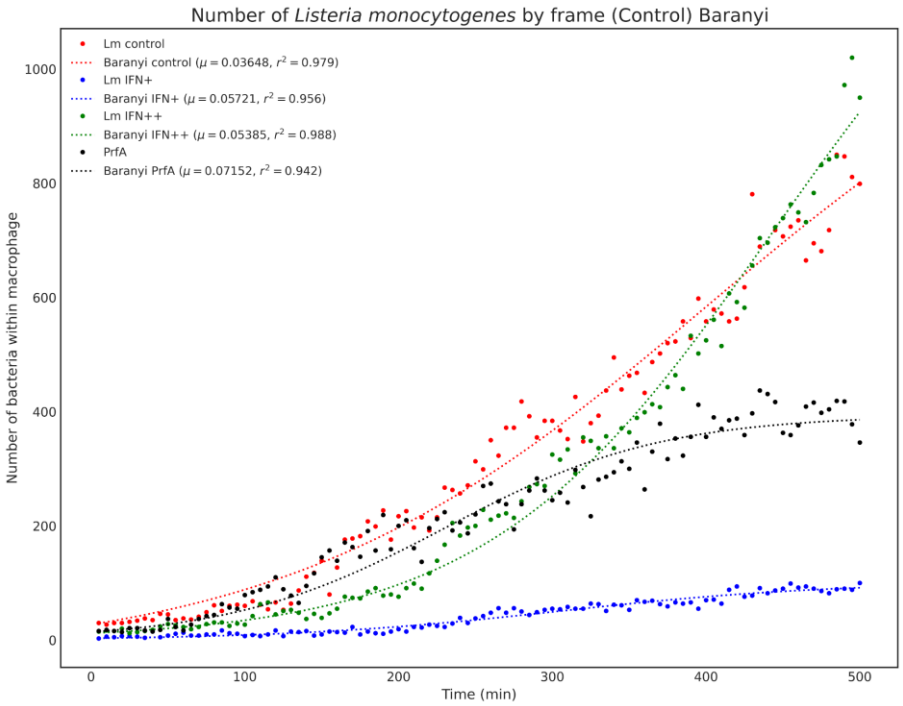


**Figure 9:** Barany modeling fourth test with control, interferon alpha, interferon alpha with doubled dose and PrfA at 500 minutes.
**Made by:** Minango María, 2023.

## Comparison of parameters in Baranyi

In research, the Baranyi model is important because of its ability to represent a variety of growth behaviors. This model is characterized by four parameters: A, u, and q which describe key aspects of growth. In addition to the parameters, the coefficient of determination R^2 is used to measure the level of fit of the models.

**Table 1:** Parameters obtained with each model in Baranyi model

| Model | A | U | q | R2 |
|---|---|---|---|---|
| Baranyi Control | 0.060 | -0.056 | 0.001 | 0.970 |
| Baranyi INF+ | 654.264 | 0.087 | 6399119.208 | 0.959 |
| Baranyi INF++ | 422.334 | 0.085 | -21352847.837 | 0.969 |
| Baranyi Control | 3252.185 | 0.020 | -1.061 | 0.962 |
| Baranyi INF+ | 347.583 | 0.069 | 5729217.839 | 0.812 |
| Baranyi INF++ | 493.817 | 0.072 | 2059447.609 | 0.865 |
| Baranyi PrfA | 116.805 | 0.070 | 5292236.361 | 0.785 |
| Baranyi Control | 1535.066 | 0.066 | 16458104.175 | 0.949 |
| Baranyi INF+ | 2743.422 | 0.066 | 7082002.065 | 0.973 |
| Baranyi INF++ | 2814.098 | 0.065 | 1.387 | 0.970 |
| Baranyi PrfA | 2466.339 | 0.063 | 5869668.873 | 0.954 |
| Baranyi Control | 1206.526 | 0.036 | -1.781 | 0.979 |
| Baranyi INF+ | 101.481 | 0.057 | 652215.614 | 0.956 |
| Baranyi INF++ | 1423.722 | 0.054 | 22963475.234 | 0.988 |
| Baranyi PrfA | 393.995 | 0.072 | 8716143.274 | 0.942 |

**Made by:** Minango María, 2023.

The remarkable results in the table show significant variations in the parameters of the Baranyi model for different experimental conditions. In the case of parameter A, a wide range of values is observed, from low values in the range of 0.060 to considerably high values such as 654.264 and 422.334 in the INF+ and INF++ conditions, respectively. The rate of change of growth rate (q) also shows a large variability, with values ranging from 0.001 to 6399119.208 in the Control and INF+ conditions, respectively. Furthermore, the coefficient of determination (R2) reflects the goodness of fit of the models, where high values consistent with modeling accuracy are evident, such as 0.970 in the Control condition and 0.988 in INF++, while other conditions show slightly lower but still acceptable values. These results underline the significant influence of experimental conditions on the parameters of the Baranyi model and highlight the importance of carefully considering these conditions when modeling microbial growth.

### Gompertz model

The analysis of bacterial growth of *L. monocytogenes* using the Gompertz model has generated significant results (**Figure 10**). Three treatments were evaluated: control, interferon alpha, and interferon alpha. The coefficients of determination (R2) obtained for each treatment were 0.975, 0.96 and 0.961 respectively, suggesting a good fit of the Gompertz model to the observed data.

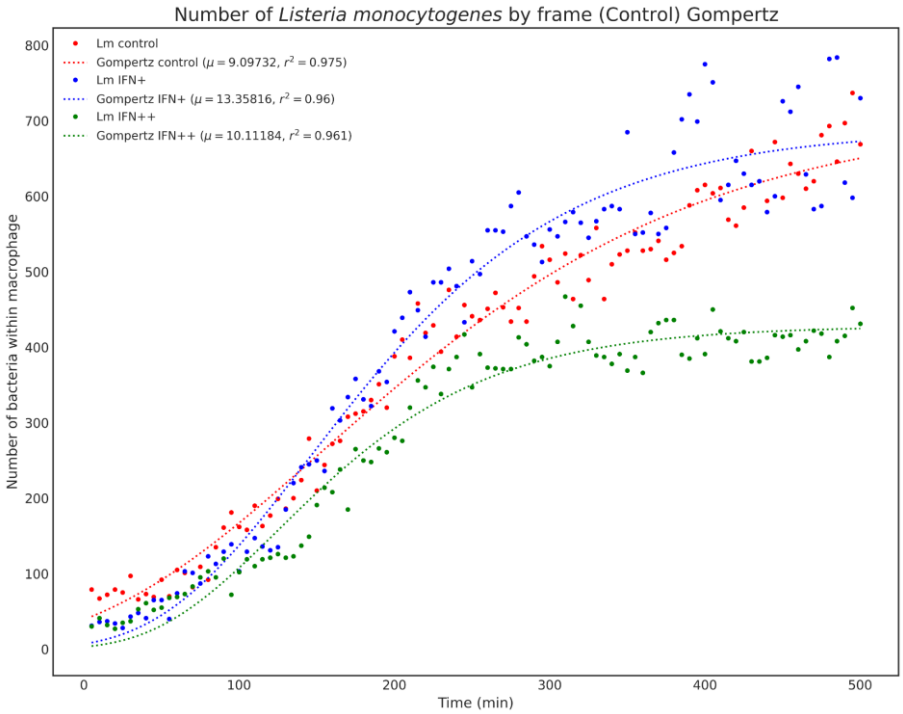


**Figure 10:** Gompertz modeling the first test with control, interferon alpha, and interferon alpha with doubled dose at 500 minutes.
**Made by:** Minango María, 2023.

Four different treatments were evaluated: control, interferon alpha, interferon alpha, and PrfA (**Figure 11**), each of which was modeled using the Gompertz approach. The coefficients of determination (R2) obtained for each treatment were 0.974, 0.99, 0.979 and 0.962, respectively.

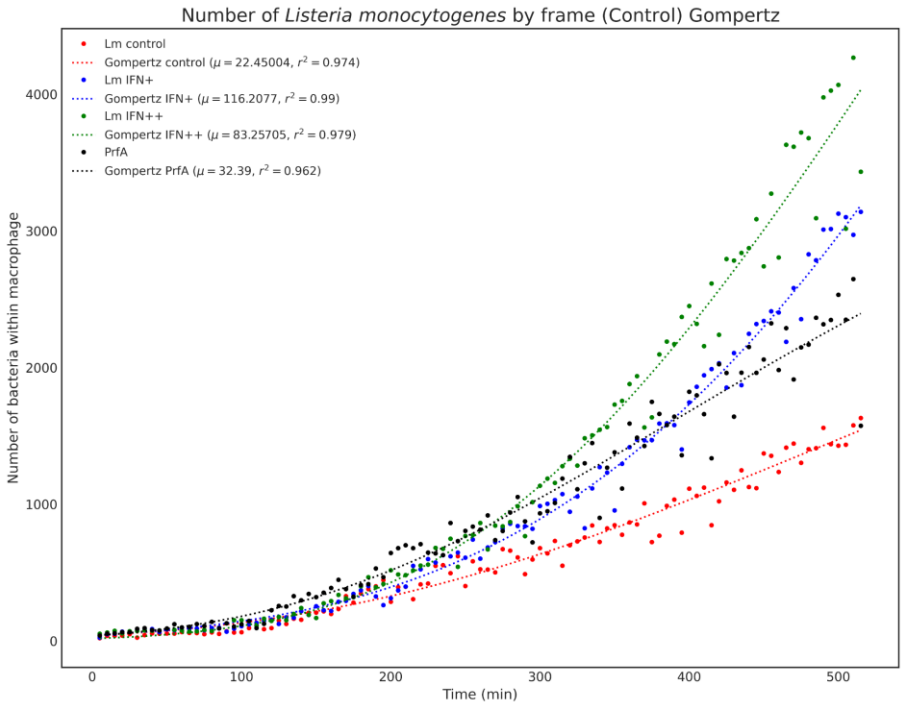


**Figure 11:** Gompertz modeling second test with control, interferon alpha, interferon alpha with doubled dose and PrfA at 500 minutes.
**Made by:** Minango María, 2023.

Four different treatments were evaluated: control, interferon alpha, interferon alpha and PrfA, and each was modeled using the Gompertz approach (**Figure 12**). The coefficients of determination (R2) obtained for each treatment were 0.96, 0.876, 0.884 and 0.895, respectively.

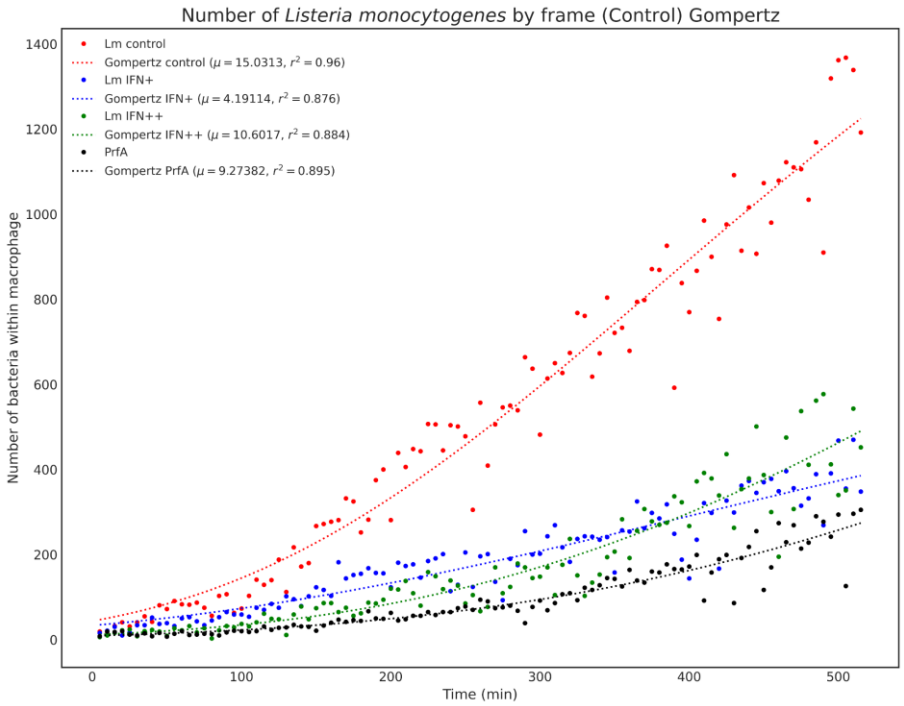


**Figure 12:** Gompertz modeling third test with control, interferon alpha, interferon alpha with doubled dose and PrfA at 500 minutes.
**Made by:** Minango María, 2023.

Four treatments were examined: control, interferon alpha, interferon alpha and PrfA (**Figura 13**). Each treatment was modeled with the Gompertz approach, and the coefficients of determination (R2) obtained were 0.98, 0.954, 0.992 and 0.961, respectively.

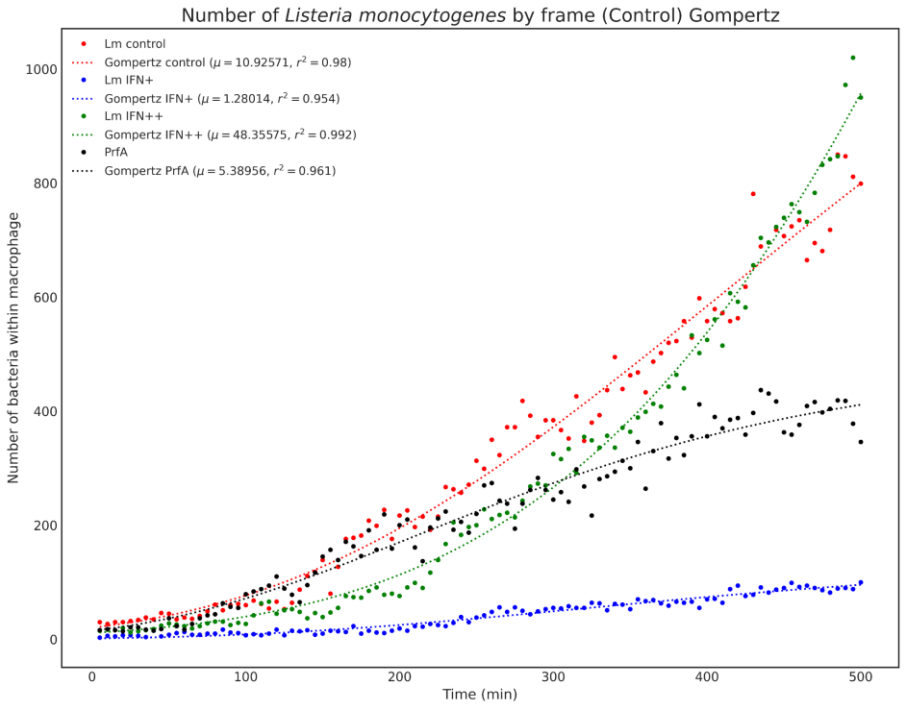


**Figure 13:** Gompertz modeling fourth test with control, interferon alpha, interferon alpha with doubled dose and PrfA at 500 minutes.
**Made by:** Minango María, 2023.

### Comparison of parameters in Gompertz

In research, the Gompertz model is important because of its ability to represent a variety of growth behaviors. This model is characterized by four parameters: A, u, and q which describe key aspects of growth. In addition to the parameters, the coefficient of determination R^2 is used to measure the level of fit of the models.

**Table 2:** Parameters obtained with each model in Gompertz.

| Model | A | u | q | R2 |
|---|---|---|---|---|
| Gompertz Control | 711.499 | 9.097 | 1.887 | 0.975 |
| Gompertz INF+ | 688.964 | 13.358 | 10.085 | 0.960 |
| Gompertz INF++ | 428.157 | 10.112 | 9.446 | 0.961 |
| Gompertz Control | 2256.399 | 15.031 | 20.583 | 0.960 |
| Gompertz INF+ | 790.728 | 4.191 | 10.671 | 0.876 |
| Gompertz INF++ | 2464.945 | 10.602 | 58.474 | 0.884 |
| Gompertz PrfA | 2904.724 | 9.274 | 86.762 | 0.895 |
| Gompertz Control | 3952.534 | 22.450 | 34.332 | 0.974 |
| Gompertz INF+ | 30278.095 | 116.208 | 84.938 | 0.990 |
| Gompertz INF++ | 13660.431 | 83.257 | 54.662 | 0.979 |
| Gompertz PrfA | 4408.286 | 32.390 | 28.181 | 0.962 |
| Gompertz Control | 1638.355 | 10.926 | 26.537 | 0.980 |
| Gompertz INF+ | 143.521 | 1.280 | 21.730 | 0.954 |
| Gompertz INF++ | 13262.607 | 48.356 | 96.623 | 0.992 |
| Gompertz PrfA | 490.869 | 5.390 | 8.448 | 0.961 |

**Made by:** Minango María, 2023.

The results obtained with the Gompertz model reveal significant diversity in the parameters for different experimental conditions. For example, parameter A, which reflects the maximum asymptotic value, varies widely from low values such as 143.521 to high values such as 30278.095 in the Control and INF+ conditions, respectively. As for parameter u, which describes the delay phase, remarkable variations are also observed, with values ranging from 1280 to 116,208 in the same conditions mentioned above. On the other hand, the parameter q, related to the rate of change of the growth rate, presents a wide dispersion, with values ranging from 1.887 to 96.623 in different experimental conditions. The coefficients of determination (R2) provide a measure of the goodness of fit of the models, showing values ranging from 0.875 to 0.992, reflecting the ability of the Gompertz model to explain the variability in the observed data. These results highlight the importance of considering experimental conditions when applying microbial growth models, since they significantly influence the parameters obtained and, therefore, the predictive capacity of the model.

## Logistical model

Analysis of bacterial growth of *Listeria monocytogenes* using the logistic growth model has yielded remarkable results (**Figure 14**). Three different treatments were evaluated: control, interferon alpha, and interferon alpha, each of which was modeled with the logistic model. The coefficients of determination (R2) obtained for each treatment were 0.97, 0.959 and 0.973, respectively.

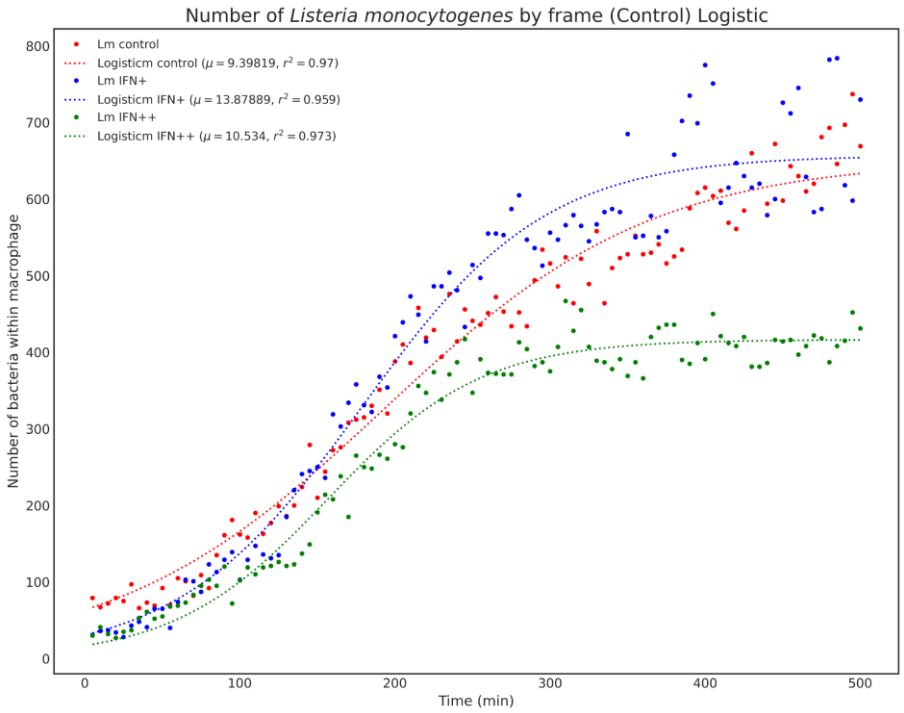


**Figure 14:** Logistic modeling the first test with control, interferon alpha, and interferon alpha with doubled dose at 500 minutes.
**Made by:** Minango María, 2023.

Four different treatments were examined: control, interferon alfa, interferon alfa and PrfA, each of which was modeled with the logistic approach (**Figure 15**). The coefficients of determination (R2) obtained for each treatment were 0.97, 0.989, 0.98 and 0.961, respectively.

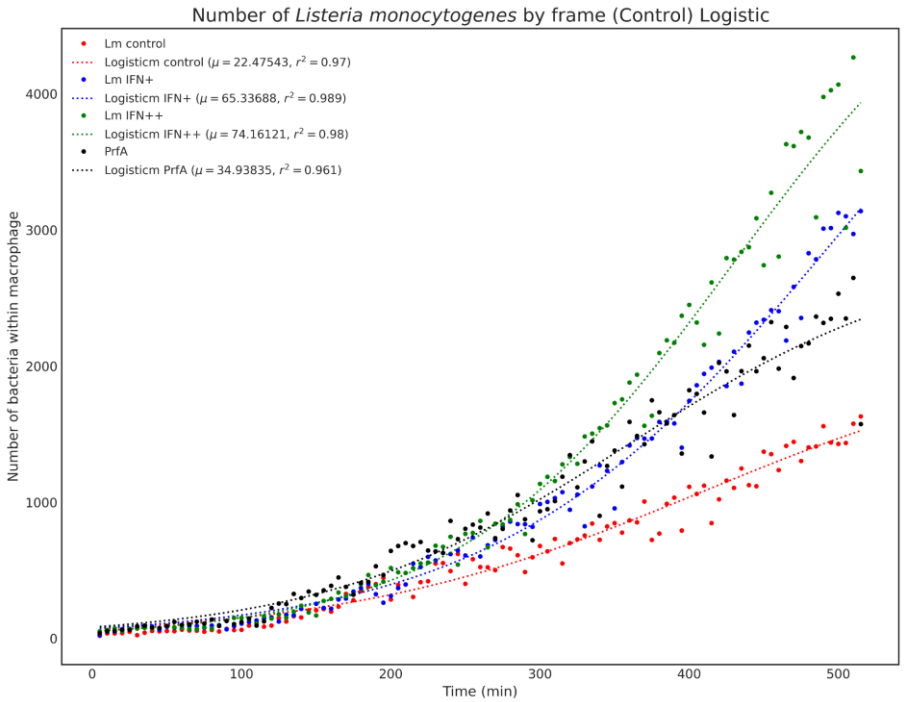


**Figure 15:** Logistic modeling with control second test, interferon alpha, interferon alpha with doubled dose and PrfA at 500 minutes.
**Made by:** Minango María, 2023.

Four different treatments were evaluated: control, interferon alfa, interferon alfa and PrfA, and each was modeled using the logistic approach (**Figure 16**). The coefficients of determination (R2) obtained for each treatment were 0.955, 0.871, 0.886 and 0.988, respectively. Although the R2 values for the interferon alpha treatments are comparatively lower than the control, they still indicate a reasonable fit of the logistic model to the observed data. On the other hand, PrfA treatment shows an exceptionally high fit.

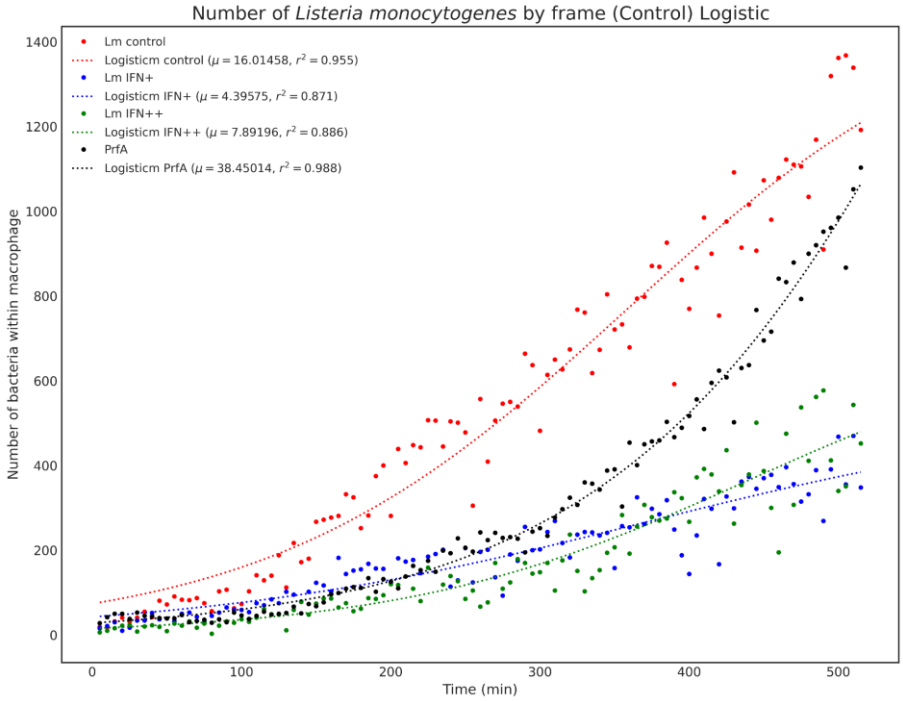


**Figure 16:** Logistic modeling third test with control, interferon alpha, interferon alpha with doubled dose and PrfA at 500 minutes.
**Made by:** Minango María, 2023.

Four different treatments were examined: control, interferon alpha, interferon alpha and PrfA (**Figura 17**). Each treatment was modeled with the Logistic approach, and the coefficients of determination (R2) obtained were 0.977, 0.956, 0.99 and 0.955, respectively.

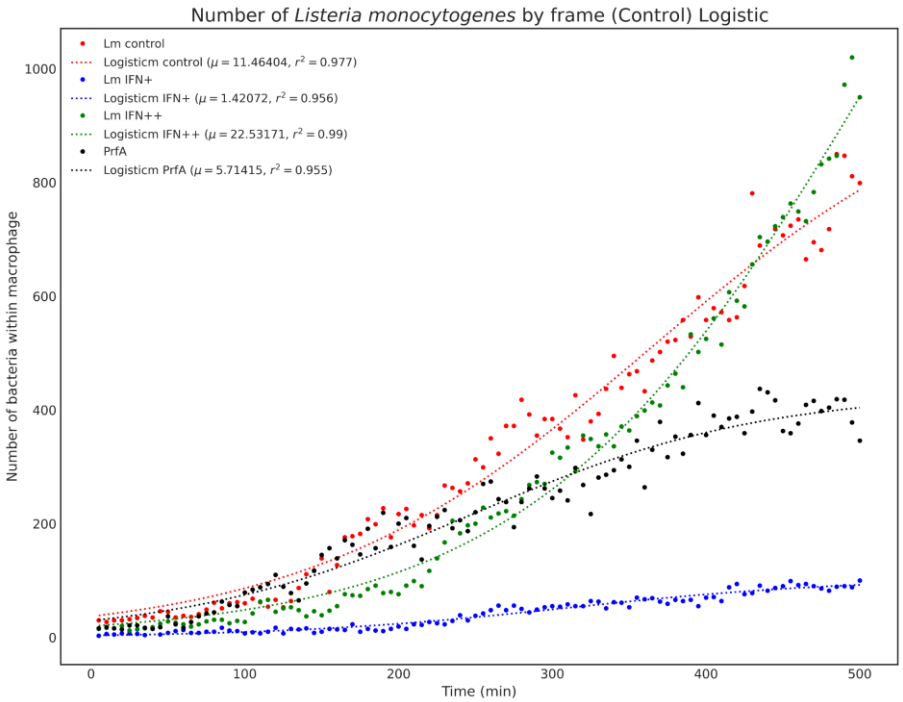


**Figure 17:** Logistic modeling fourth test with control, interferon alpha, interferon alpha with doubled dose and PrfA at 500 minutes.
**Made by:** Minango María, 2023.

## Comparison of parameters in Logistic model

In research, the Logistic model is important because of its ability to represent a variety of growth behaviors. This model is characterized by four parameters: A, u, and q which describe key aspects of growth. In addition to the parameters, the coefficient of determination R2 is used to measure the level of fit of the models.

**Table 3:** Parameters obtained with each model in the Logistic model

| Model | A | u | Q | R2 |
|---|---|---|---|---|
| Logistic Control | 651.595 | 9.398 | 36.597 | 0.970 |
| Logistic INF+ | 656.933 | 13.879 | 33.738 | 0.959 |
| Logistic INF++ | 416.393 | 10.534 | 29.345 | 0.973 |
| Logistic Control | 1536.053 | 16.015 | 69.646 | 0.955 |
| Logistic INF+ | 535.074 | 4.396 | 72.523 | 0.871 |
| Logistic INF++ | 724.634 | 7.892 | 85.631 | 0.886 |
| Logistic PrfA | 4037.409 | 38.450 | 127.969 | 0.988 |
| Logistic Control | 2158.949 | 22.475 | 79.881 | 0.970 |
| Logistic INF+ | 5957.201 | 65.337 | 98.259 | 0.989 |
| Logistic INF++ | 5486.178 | 74.161 | 83.775 | 0.980 |
| Logistic PrfA | 2857.005 | 34.938 | 69.969 | 0.961 |
| Logistic Control | 1018.044 | 11.464 | 70.822 | 0.977 |
| Logistic INF+ | 103.818 | 1.421 | 60.030 | 0.956 |
| Logistic INF++ | 2003.197 | 22.532 | 100.255 | 0.990 |
| Logistic PrfA | 431.846 | 5.714 | 47.519 | 0.955 |

**Made by:** Minango María, 2023.

The results obtained using the logistic model (**Table 3**) reveal remarkable variations in the parameters for different experimental conditions. For example, parameter A, which represents the upper limit of the population, varies from low values such as 103.818 to high values such as 5957.201 in the control and INF+ conditions, respectively. Regarding parameter u, which indicates the maximum growth rate, significant differences are also observed, with values ranging from 1,421 to 74,161 under the same conditions mentioned above. On the other hand, the parameter q, related to the rate of change of the growth rate, presents a wide dispersion, with values ranging from 29.345 to 127.969 in different experimental conditions. The coefficients of determination (R2) provide a measure of the goodness of fit of the models, showing values ranging from 0.855 to 0.990, reflecting the ability of the logistic model to explain the variability in the observed data. These results underscore the crucial influence of experimental conditions on the parameters obtained and the need to consider them carefully when applying microbial growth models.

### Richards model

Bacterial growth models make varying fits to the data, and each treatment exhibits specific dynamics depending on the model employed (**Figure 18**). The coefficient of determination (R2) indicates the fit's quality, and each model's particular parameters provide details on the speed, upper limit, and shape of the growth curve in the context of the treatments applied to *L. monocytogenes*.

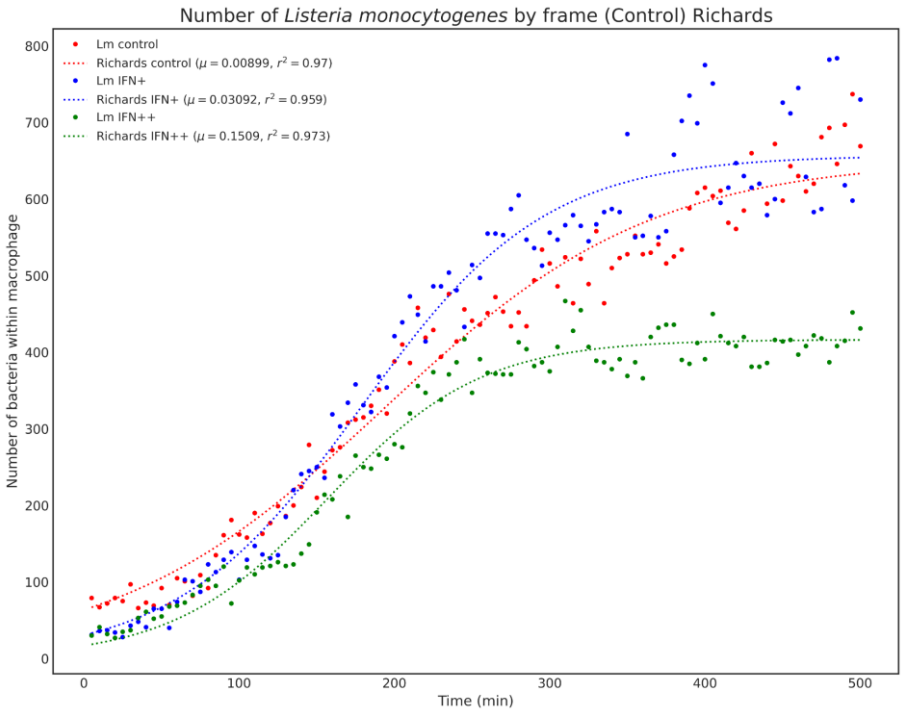


**Figure 18:** Richards modeling the first test with control, interferon alpha, and interferon alpha with doubled dose at 500 minutes.
**Made by:** Minango María, 2023.

Four different treatments were examined: control, interferon alfa, interferon alfa and PrfA, each of which was modeled with the Richards approach (**Figure 19**). The coefficients of determination (R2) obtained for each treatment were 0.97, 0.989, 0.98 and 0.961, respectively.

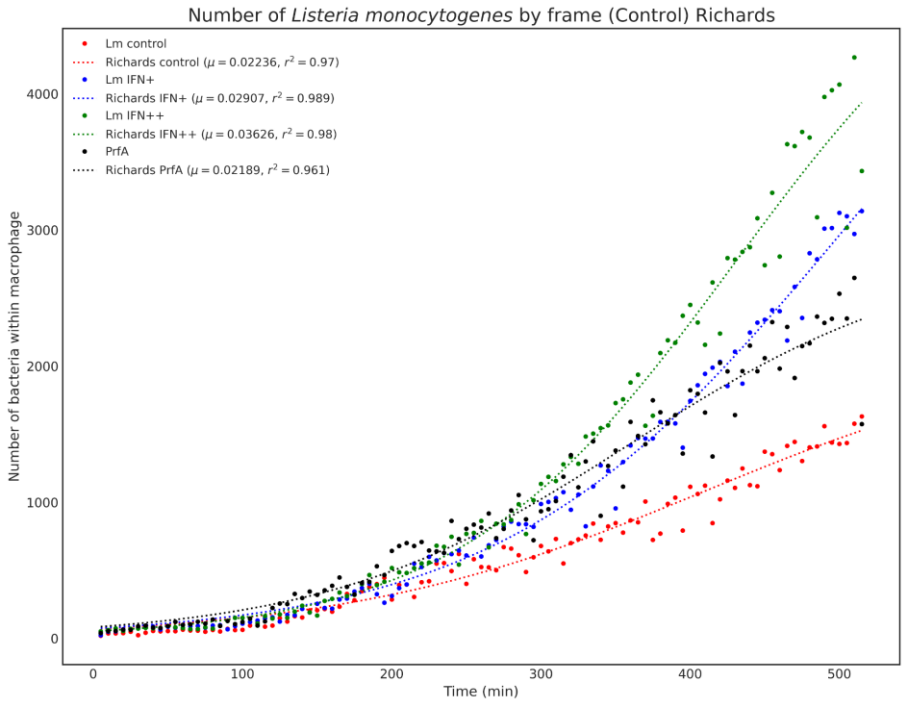


**Figure 19:** Richards modeling second test with control, interferon alpha, interferon alpha with doubled dose and PrfA at 500 minutes.
**Made by:** Minango María, 2023.

Four different treatments were evaluated: control, interferon alpha, interferon alpha and PrfA (**Figure 20**). Each treatment was modeled using the Richards approach, and the coefficients of determination (R2) obtained were 0.955, 0.871, 0.886 and 0.988, respectively.

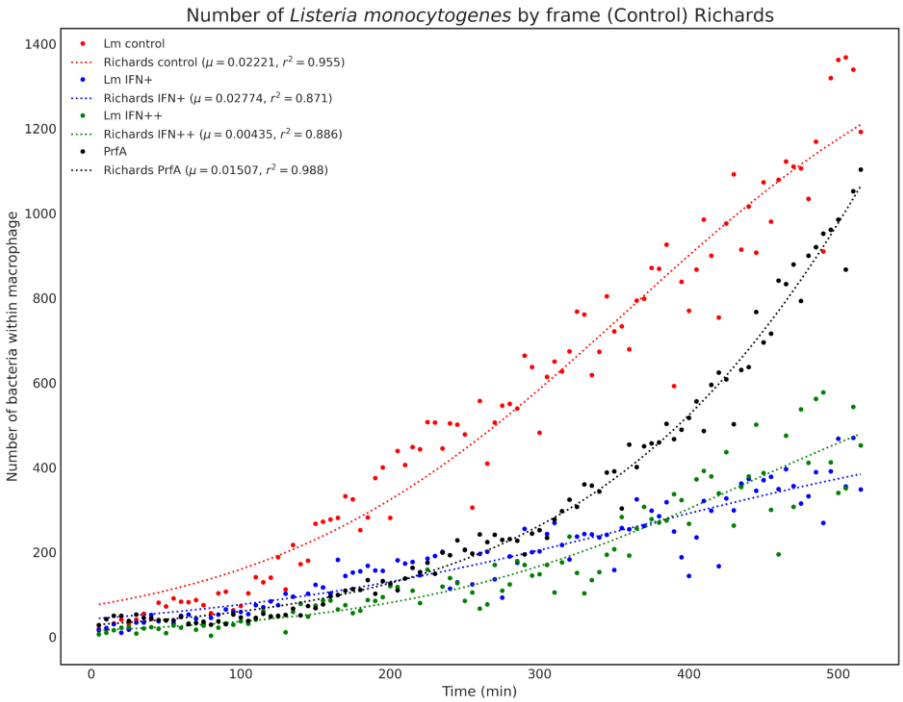


**Figure 20:** Richards modeling third test with control, interferon alpha, interferon alpha with doubled dose and PrfA at 500 minutes.
**Made by:** Minango María, 2023.

Four different treatments were examined: control, interferon alpha, interferon alpha and PrfA (**Figura 21**). Each treatment was modeled with the Gompertz approach, and the coefficients of determination (R2) obtained were 0.977, 0.956, 0.99 and 0.955, respectively.

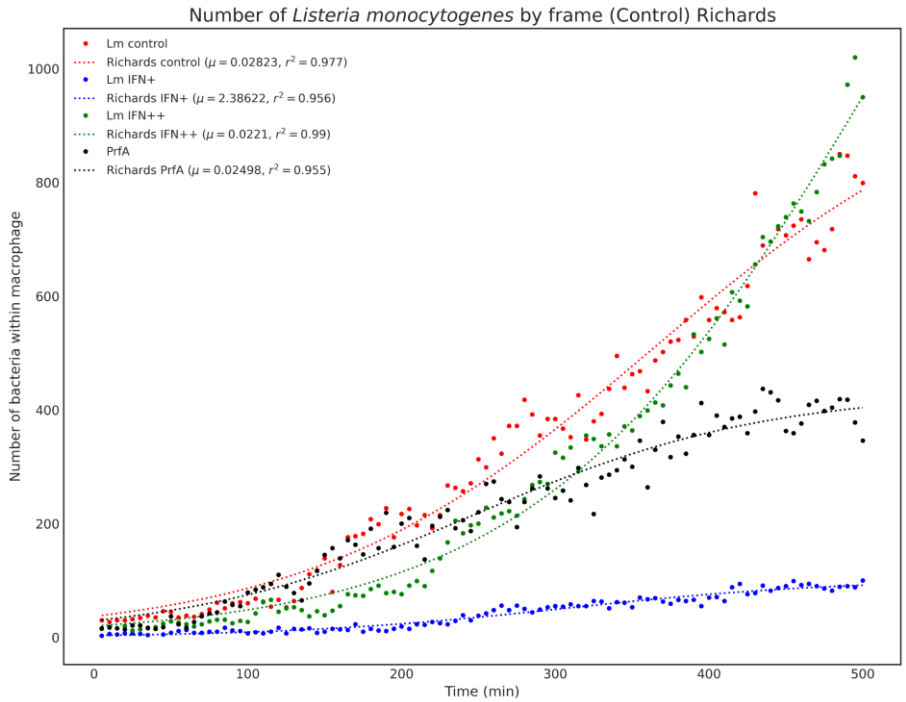


**Figure 21:** Richards modeling fourth test with control, interferon alpha, interferon alpha with doubled dose and PrfA at 500 minutes.
**Made by:** Minango María, 2023.

### Comparison of parameters in the Richards model

In research, the Richards model is important because it represents various growth behaviors. This model is characterized by four parameters: A, u, and q, which describe key growth aspects. In addition to the parameters, the coefficient of determination R^2 is used to measure the level of fit of the models.

**Table 4:** Parameters obtained with each model in the Richards model

| Model | A | u | q | R2 | v |
|---|---|---|---|---|---|
| Richards Control | 10.236 | 0.009 | 92.982 | 0.970 | 0.016 |
| Richards INF+ | 15.880 | 0.031 | 67.668 | 0.959 | 0.024 |
| Richards INF++ | 26.504 | 0.151 | 48.052 | 0.973 | 0.064 |
| Richards Control | 29.147 | 0.022 | 142.279 | 0.955 | 0.019 |
| Richards INF+ | 22.129 | 0.028 | 139.754 | 0.871 | 0.041 |
| Richards INF++ | 8.610 | 0.004 | 166.158 | 0.886 | 0.012 |
| Richards PrfA | 40.371 | 0.015 | 224.348 | 0.988 | 0.010 |
| Richards Control | 34.651 | 0.022 | 156.964 | 0.970 | 0.016 |
| Richards INF+ | 63.502 | 0.029 | 180.736 | 0.989 | 0.011 |
| Richards INF++ | 61.342 | 0.036 | 150.193 | 0.980 | 0.011 |
| Richards PrfA | 36.212 | 0.022 | 140.565 | 0.961 | 0.013 |
| Richards Control | 25.900 | 0.028 | 131.563 | 0.977 | 0.025 |
| Richards INF+ | 186.807 | 2.386 | 0.028 | 0.956 | 1.825 |
| Richards INF++ | 31.869 | 0.022 | 171.711 | 0.990 | 0.016 |
| Richards PrfA | 14.766 | 0.025 | 93.758 | 0.955 | 0.034 |

**Made by:** Minango María, 2023.

The results obtained with the Richards model show a wide variability in the parameters for different experimental conditions. For example, parameter A, which represents the maximum value of the population, varies from low values such as 8,610 to high values such as 186,807 in the INF++ and INF+ conditions, respectively. As for parameter u, which describes the maximum growth rate, significant differences are also observed, with values ranging from 0.004 to 2.386 in different experimental conditions. On the other hand, parameter q, related to the rate of change of the growth rate, shows a wide dispersion, with values ranging from 48.052 to 224.348 in different experimental conditions. In addition, the parameter v, which influences the curvature of the growth function, also varies markedly between conditions. The coefficients of determination (R2) provide a measure of the goodness of fit of the models, showing values ranging from 0.871 to 0.990, reflecting the ability of the Richards model to explain the variability in the observed data.

## Statistical analysis Statistical analysis by Bayesian information criterion (BIC)

**Table 5:** Bayesian information criterion

| Model | Treatment | BIC |
|---|---|---|
| Baranyi | Control | -1.316 |
| Baranyi | INF+ | 2.582 |
| Baranyi | INF++ | -2.067 |
| Baranyi | Control | 7.440 |
| Baranyi | INF+ | 8.934 |
| Baranyi | INF++ | -22.167 |
| Baranyi | PrfA | -17.216 |
| Baranyi | Control | 10.948 |
| Baranyi | INF+ | -16.565 |
| Baranyi | INF++ | 26.754 |
| Baranyi | PrfA | 43.766 |
| Baranyi | Control | -2.941 |
| Baranyi | INF+ | 13.487 |
| Baranyi | INF++ | 1.393 |
| Baranyi | PrfA | 29.015 |
| Gompertz | Control | -1.660 |
| Gompertz | INF+ | 5.465 |
| Gompertz | INF++ | -13.133 |
| Gompertz | Control | -3.422 |
| Gompertz | INF+ | -26.402 |
| Gompertz | INF++ | 16.764 |
| Gompertz | PrfA | 3.357 |
| Gompertz | Control | 15.747 |
| Gompertz | INF+ | 13.174 |
| Gompertz | INF++ | 28.038 |
| Gompertz | PrfA | -0.250 |
| Gompertz | Control | -5.967 |
| Gompertz | INF+ | 2.386 |
| Gompertz | INF++ | 20.019 |
| Gompertz | PrfA | 8.802 |
| Logistic | Control | 3.206 |
| Logistic | INF+ | 22.016 |
| Logistic | INF++ | 1.193 |
| Logistic | Control | -9.748 |

| | | |
|---|---|---|
| Logistic | INF+ | -18.333 |
| Logistic | INF++ | 8.629 |
| Logistic | PrfA | 0.747 |
| Logistic | Control | -7.198 |
| Logistic | INF+ | 34.241 |
| Logistic | INF++ | 20.020 |
| Logistic | PrfA | -2.078 |
| Logistic | Control | 34.265 |
| Logistic | INF+ | -12.250 |
| Logistic | INF++ | 30.827 |
| Logistic | PrfA | 4.270 |
| Richards | Control | 20.105 |
| Richards | INF+ | 2.152 |
| Richards | INF++ | -6.945 |
| Richards | Control | -12.444 |
| Richards | INF+ | 0.963 |
| Richards | INF++ | -9.260 |
| Richards | PrfA | 15.035 |
| Richards | Control | -9.983 |
| Richards | INF+ | 19.206 |
| Richards | INF++ | 23.790 |
| Richards | PrfA | 10.854 |
| Richards | Control | 2.310 |
| Richards | INF+ | 4.270 |
| Richards | INF++ | 5.878 |
| Richards | PrfA | -2.597 |

**Made by:** Minango María, 2023.

The models generally have BIC values that vary considerably between model specifications. Some variants have negative BIC values, indicating a good fit of the model to the data with a low complexity penalty. However, other models have positive BIC values, suggesting that they may be less appropriate in fit and complexity. Gompertz models exhibit a range of BIC values. Some models have relatively low BIC values, such as -26.402, suggesting a good fit to the data with reasonable complexity. On the other hand, some models exhibit higher BIC values, suggesting a less optimal fit or greater model complexity. The Baranyi models also show a variety of BIC values. Some models have relatively low BIC values, such as -22.167, suggesting an excellent fit to the data with reasonable complexity. On the other hand, some models exhibit

higher BIC values, suggesting a less optimal fit or greater model complexity. Logistic models exhibit a range of BIC values. Some models have relatively low BIC values, such as -18.333, suggesting an excellent fit to the data with moderate complexity. However, other models exhibit higher BIC values, indicating potentially less optimal fit or higher complexity.

## DISCUSSION

The study addresses the bacterial growth of *Listeria monocytogenes* under various treatments using different growth models.

### Analysis of the Baranyi Model

To analyze bacterial growth of *Listeria monocytogenes*, four treatments were used: Control, INF+ (Interferon alpha), INF++ (Interferon alpha doubled the dose) and PrfA. The parameters used for each model were the maximum value of the bacterial population (A), the growth rate (u) and the adaptation rate (q).

In general (**Table 1**), it is observed that treatments with interferon alpha (INF+ and INF++) have a significant effect on the bacterial population, since they present lower maximum bacterial population values than the control and PrfA. Furthermore, the growth rate (u) is lower in treatments with interferon alfa, indicating that the bacteria grow more slowly in the presence of interferon alfa (George et al., 2012). On the other hand, treatment with PrfA presents a maximum value of bacterial population higher than the control and treatments with interferon alpha, and it is shown that PrfA promotes bacterial growth because PrfA is a master regulator that controls the expression of several genes of virulence in *L. monocytogenes*, allowing it to survive and grow within host cells. This protein is essential for the pathogenicity of *L. monocytogenes*, as it regulates the expression of genes involved in cell invasion, phagosome escape, and stress resistance (Muñiz, 2018).

As for the adaptation rate (q), it is observed that the values are very high in all interferon-alpha thing and the bacterium is rapidly adapting to the environmental conditions (Iharilalao Dubail et al., 2000). However, the q values are exceptionally high in the interferon-alpha treatments, suggesting that the bacterium may be actively fighting against interferon-alpha.

**Analysis of the Gompertz Model**

Adaptation rates also increase with interferon-alpha treatment, indicating that bacteria can develop strategies to adapt and survive in interferon-alpha. On the other hand, PrfA treatment shows wide parameter variability and relatively high maximum bacterial population values compared to interferon-alpha treatments. Growth and adaptation rates are variable, suggesting that the bacteria may respond diversely to the presence of PrfA, possibly adapting to the treatment conditions. The control treatment shows consistently high maximum bacterial population values compared to the interferon alfa and PrfA treatments. Growth and adaptation rates are also high in the control treatment, suggesting that the bacteria can thrive without specific treatments.

Contrasting the different treatments, it appears that interferon alpha, especially at higher doses (INF++), can have a significant effect in reducing the bacterial growth of *Listeria monocytogenes*. On the other hand, PrfA treatment appears to have a less consistent influence on reducing bacterial growth compared to interferon alfa. The control treatment, for its part, allows unrestricted bacterial growth.

**Analysis of the Logistic Model**

The control treatment represents standard conditions without specific intervention. The maximum bacterial population (A) values under control vary considerably, possibly due to inherent variations in experimental conditions or unknown factors that may affect bacterial growth. The growth (u) and adaptation (q) rates under control are moderate compared to the interferon alfa and interferon alfa duplicate treatments. This suggests that standard conditions provide a relatively stable growth environment for *Listeria monocytogenes* but do not stimulate excessive bacterial growth (Ferreira et al., 2014).

In most cases, both INF+ and INF++ show an increase in the maximum value of the bacterial population (A) compared to the control. This suggests that interferon alfa, either in standard or doubled doses, may promote the growth of *Listeria monocytogenes* (Demiroz et al., 2021). The growth (u) and adaptation (q) rates are higher in treatments with interferon alpha, indicating a greater capacity for reproduction and adaptation of bacteria under the influence of this compound. The variability in A, u, and q values may reflect the sensitivity of *Listeria monocytogenes* to different concentrations of interferon

alfa, suggesting that higher doses may have an even more significant impact on bacterial growth (George et al., 2012).

PrfA treatment also shows an increase in the maximum bacterial population value compared to the control in most cases, although the variability is greater in this treatment. Growth and adaptation rates under PrfA are variable, suggesting that this treatment may have divergent effects on the proliferation and adaptation of *Listeria monocytogenes* under different experimental conditions. The high variability in A, u, and q values may indicate a more complex response of *Listeria monocytogenes* to PrfA treatment, which could be due to the interaction of this compound with multiple metabolic pathways or cellular processes (de las Heras et al., 2011).

**Analysis of the Richards Model**

The INF+ treatment generally shows a higher maximum bacterial population value (A) than the control (**Table 4**). The growth rate (u) under INF+ tends to be higher than in the control. The adaptation rate (q) also tends to be higher in INF+ compared to control. These results suggest that interferon alpha treatment can stimulate bacterial growth compared to the control. INF++ tends to have lower A values compared to the control in most cases. The growth rate (u) can vary considerably in INF++, suggesting a non-linear response to increasing interferon alfa dose. The adaptation rate (q) also tends to vary significantly in INF++ compared to the control. These findings suggest that treatment with a doubled dose of interferon alfa may have inhibitory effects on bacterial growth compared to the contro (Demiroz et al., 2021)l.

PrfA tends to show higher A values compared to the control in most cases. The growth rate (u) in PrfA tends to be lower than in the control. The adaptation rate (q) can vary, but tends to be lower in PrfA compared to the control. These results (**Table 4**) suggest that PrfA treatment can promote bacterial growth compared to the control, but with a slower growth rate and possibly a lower adaptive capacity. The INF+ and PrfA treatments appear to stimulate bacterial growth compared to the control, although with different mechanisms and growth profiles. Meanwhile, INF++ tends to have an inhibitory effect on bacterial growth compared to the control, possibly due to a non-linear response to interferon alpha dose.

**Best model for *Listeria monocytogenes***

**Table 6.** Parameters with the best Bayesian Information Criterion

| Model | Treatment | BIC |
|---|---|---|
| Gompertz | INF+ | -26.402 |

**Made by:** Minango María, 2023.

The best adjustment that has occurred has been Gompertz with the Interferon alpha treatment.

This model divides microbial growth into three stages: the lag phase, the exponential phase and the stationary phase. The lag phase is the time it takes for the bacteria to adapt to the environment in which it has been planted, the exponential phase is when the bacteria reproduces rapidly and the stationary phase is when the bacterial population stabilizes due to lack of nutrients. With the adjustment that has been made, it has been seen that the data have been better coupled to the Gompertz model. Likewise, this has been compared with other mathematical models and has been shown to be one of the best for modeling and predicting the growth of *Listeria monocytogenes.*

## CONCLUSIONS

The study analyzed the growth of *Listeria monocytogenes* under different treatments using four mathematical models: Baranyi, Gompertz, Logistic and Richards. The parameters used for each model were the maximum value of the bacterial population, the growth rate and the adaptation rate. The results showed that interferon alpha treatments had a significant effect on reducing bacterial growth, while PrfA treatment promoted bacterial growth. The control treatment allowed unrestricted bacterial growth. The Gompertz model was found to be the best model for predicting the growth of *Listeria monocytogenes* under interferon alfa treatment. The study provides accurate predictive models for the growth of *L. monocytogenes* that can be used in shelf-life and microbial safety assessments of food products.

## REFERENCES


Allerberger, F., & Wagner, M. (2010). Listeriosis: A resurgent foodborne infection. *Clinical Microbiology and Infection*, *16*(1), 16–23. https://doi.org/10.1111/j.1469-0691.2009.03109.x

Aubry, C., Corr, S. C., Wienerroither, S., Goulard, C., Jones, R., Jamieson, A. M., Decker, T., O'Neill, L. A. J., Dussurget, O., & Cossart, P. (2012). Both TLR2 and TRIF Contribute to Interferon-β Production during Listeria Infection. *PLOS ONE*, *7*(3), e33299. https://doi.org/10.1371/journal.pone.0033299

Bankhead, P. (2014). *Analyzing fluorescence microscopy images with ImageJ*. 195.

Brian Henderson & Andrew Martin. (2011). *Bacterial Virulence in the Moonlight: Multitasking Bacterial Moonlighting Proteins Are Virulence Determinants in Infectious Disease | Infection and Immunity*. https://journals.asm.org/doi/10.1128/iai.00179-11

Brinkmann, V., Reichard, U., Goosmann, C., Fauler, B., Uhlemann, Y., Weiss, D. S., Weinrauch, Y., & Zychlinsky, A. (2004). Neutrophil extracellular traps kill bacteria. *Science (New York, N.Y.)*, *303*(5663), 1532–1535. https://doi.org/10.1126/science.1092385

Cossart, P., Pizarro-Cerdá, J., & Lecuit, M. (2003). Invasion of mammalian cells by *Listeria monocytogenes*: Functional mimicry to subvert cellular functions. *Trends in Cell Biology*, *13*(1), 23–31. https://doi.org/10.1016/S0962-8924(02)00006-5

de las Heras, A., Cain, R. J., Bielecka, M. K., & Vázquez-Boland, J. A. (2011). Regulation of Listeria virulence: PrfA master and commander. *Current Opinion in Microbiology*, *14*(2), 118–127. https://doi.org/10.1016/j.mib.2011.01.005

Demiroz, D., Platanitis, E., Bryant, M., Fischer, P., Prchal-Murphy, M., Lercher, A., Lassnig, C., Baccarini, M., Müller, M., Bergthaler, A., Sexl, V., Dolezal, M., & Decker, T. (2021). *Listeria monocytogenes* infection rewires host metabolism with regulatory input from type I interferons. *PLOS Pathogens*, *17*(7), e1009697. https://doi.org/10.1371/journal.ppat.1009697

Elisia, I., Pae, H. B., Lam, V., Cederberg, R., Hofs, E., & Krystal, G. (2018). Comparison of RAW264.7, human whole blood and PBMC assays to screen for immunomodulators. *Journal of Immunological Methods*, *452*, 26–31. https://doi.org/10.1016/j.jim.2017.10.004

Espinosa-Mata, E., Mejía, L., Villacís, J. E., Alban, V., & Zapata, S. (2022). Detection and genotyping of *Listeria monocytogenes* in artisanal soft cheeses from Ecuador. *Revista Argentina de Microbiología*, *54*(1), 53–56. https://doi.org/10.1016/j.ram.2021.02.013

Ferreira, V., Wiedmann, M., Teixeira, P., & Stasiewicz, M. J. (2014). *Listeria monocytogenes* Persistence in Food-Associated Environments: Epidemiology, Strain Characteristics, and Implications for Public Health. *Journal of Food Protection*, *77*(1), 150–170. https://doi.org/10.4315/0362-028X.JFP-13-150

Flannagan, R. S., Cosío, G., & Grinstein, S. (2009). Antimicrobial mechanisms of phagocytes and bacterial evasion strategies. *Nature Reviews Microbiology*, *7*(5), Article 5. https://doi.org/10.1038/nrmicro2128

Garzón, B. (2011). *Efectos biológicos y caracterización de dianas de la prostaglandina A1: Interacciones con proteínas de filamentos intermedios*. https://digital.csic.es/handle/10261/44466

George, P. M., Badiger, R., Alazawi, W., Foster, G. R., & Mitchell, J. A. (2012). Pharmacology and therapeutic potential of interferons. *Pharmacology & Therapeutics*, *135*(1), 44–53. https://doi.org/10.1016/j.pharmthera.2012.03.006

Gonzalez Cuello, R. E., Taron Dunoyer, A. A., & Perez Mendoza, J. (2022). Modelo de crecimiento

microbiano para predecir el comportamiento de Salmonella spp. En queso costeño colombiano. *Información tecnológica*, *33*(1 (Febrero)), 225–234.

Hilbe, J. (2017). *The statistical analysis of count data / El análisis estadístico de los datos de recuento*. https://www.tandfonline.com/doi/full/10.1080/11356405.2017.1368162

Iharilalao Dubail, Patrick Berche, The European Listeria Genome Consortium, & Alain Charbit. (2000). *Listeriolysin O as a Reporter To Identify Constitutive and In Vivo-Inducible Promoters in the Pathogen Listeria monocytogenes | Infection and Immunity*. https://journals.asm.org/doi/10.1128/iai.68.6.3242-3250.2000

InvivoGen. (2016, noviembre 25). *RAW 264.7 macrophages cell lines*. InvivoGen. https://www.invivogen.com/raw-cell-lines

Jung, S., Unutmaz, D., Wong, P., Sano, G.-I., De los Santos, K., Sparwasser, T., Wu, S., Vuthoori, S., Ko, K., Zavala, F., Pamer, E. G., Littman, D. R., & Lang, R. A. (2002). In vivo depletion of CD11c+ dendritic cells abrogates priming of CD8+ T cells by exogenous cell-associated antigens. *Immunity*, *17*(2), 211–220. https://doi.org/10.1016/s1074-7613(02)00365-5

Kaufmann, S. H. (1993). Immunity to intracellular bacteria. *Annual Review of Immunology*, *11*, 129–163. https://doi.org/10.1146/annurev.iy.11.040193.001021

Khan, T. A., Wang, X., & Maynard, J. A. (2016). Inclusion of an RGD Motif Alters Invasin Integrin-Binding Affinity and Specificity. *Biochemistry*, *55*(14), 2078–2090. https://doi.org/10.1021/acs.biochem.5b01243

Lasa, I., Pozo, J. L. del, Penadés, J. R., & Leiva, J. (2005). Biofilms bacterianos e infección. *Anales del Sistema Sanitario de Navarra*, *28*(2), 163–175.

Maria Fátima Horta, Luciana Oliveira Andrade, Érica Santos Martins-Duarte, & Thiago Castro-Gomes. (2020). *Cell invasion by intracellular parasites – the many roads to infection | Journal of Cell Science | The Company of Biologists*. https://journals.biologists.com/jcs/article/133/4/jcs232488/223966/Cell-invasion-by-intracellular-parasites-the-many

McQuin, C., Goodman, A., Chernyshev, V., Kamentsky, L., Cimini, B. A., Karhohs, K. W., Doan, M., Ding, L., Rafelski, S. M., Thirstrup, D., Wiegraebe, W., Singh, S., Becker, T., Caicedo, J. C., & Carpenter, A. E. (2018). CellProfiler 3.0: Next-generation image processing for biology. *PLOS Biology*, *16*(7), e2005970. https://doi.org/10.1371/journal.pbio.2005970

Miner, M. D., Port, G. C., & Freitag, N. E. (2007). Regulation of *Listeria monocytogenes* Virulence Genes. En H. Goldfine & H. Shen (Eds.), *Listeria monocytogenes: Pathogenesis and Host Response* (pp. 139–158). Springer US. https://doi.org/10.1007/978-0-387-49376-3_7

Muñiz, A. A. (2018). *Métodos de detección y control de Listeria monocytogenes en la industria alimentaria*.

Nag, V. L., & Kalita, J. M. (2022). Epidemiology of Parasitic Infections. En S. C. Parija & A. Chaudhury (Eds.), *Textbook of Parasitic Zoonoses* (pp. 51–58). Springer Nature. https://doi.org/10.1007/978-981-16-7204-0_6

*NIH Image to ImageJ: 25 años de análisis de imágenes | Métodos de la naturaleza*. (s/f). Recuperado el 6 de febrero de 2024, de https://www.nature.com/articles/nmeth.2089

Ohya, K., Matsumura, T., Itchoda, N., Ohashi, K., Onuma, M., & Sugimoto, C. (2003). Protective Effect of Orally Administered Human Interferon (HuIFN)-α against Systemic *Listeria monocytogenes* Infection and a Practical Advantage of HuIFN-α Derived from Transgenic Potato Plant. En I. K. Vasil (Ed.), *Plant Biotechnology 2002 and Beyond: Proceedings of the 10th IAPTC&B Congress*

*June 23–28, 2002 Orlando, Florida, U.S.A.* (pp. 389–391). Springer Netherlands. https://doi.org/10.1007/978-94-017-2679-5_79

Orsi, R. H., Bakker, H. C. den, & Wiedmann, M. (2011). *Listeria monocytogenes* lineages: Genomics, evolution, ecology, and phenotypic characteristics. *International Journal of Medical Microbiology*, *301*(2), 79–96. https://doi.org/10.1016/j.ijmm.2010.05.002

Pizarro-Cerdá, J., Kühbacher, A., & Cossart, P. (2012). Entry of *Listeria monocytogenes* in mammalian epithelial cells: An updated view. *Cold Spring Harbor Perspectives in Medicine*, *2*(11), a010009. https://doi.org/10.1101/cshperspect.a010009

Reguera, J. I. (1995). *Infección alimentaria por Listeria monocytogenes*.

Sánchez, D. (2014). *Análisis del software ImageJ para el análisis científico de imágenes*.

Schindelin, J. (2012). *Fiji: An open-source platform for biological-image analysis: Vol. 9(7)* (pp. 676–682). https://doi.org/10.1038/nmeth.2019

Southwick, F. S., & Purich, D. L. (1996). Intracellular Pathogenesis of Listeriosis. *New England Journal of Medicine*, *334*(12), 770–776. https://doi.org/10.1056/NEJM199603213341206

Stirling, D. R., Swain-Bowden, M. J., Lucas, A. M., Carpenter, A. E., Cimini, B. A., & Goodman, A. (2021). CellProfiler 4: Improvements in speed, utility and usability. *BMC Bioinformatics*, *22*(1), 433. https://doi.org/10.1186/s12859-021-04344-9

Sura A. Abdulateef, Hasan A. Aal Owaif, & Mohanad H. Hussein. (2023). *Importance of Virulence Factors in Bacterial Pathogenicity: A Review | International Journal of Medical Science and Clinical Research Studies*. https://ijmscr.org/index.php/ijmscrs/article/view/737

Theriot, J. A., Mitchison, T. J., Tilney, L. G., & Portnoy, D. A. (1992). The rate of actin-based motility of intracellular *Listeria monocytogenes* equals the rate of actin polymerization. *Nature*, *357*(6375), Article 6375. https://doi.org/10.1038/357257a0

Tjørve, K. M. C., & Tjørve, E. (2017). The use of Gompertz models in growth analyses, and new Gompertz-model approach: An addition to the Unified-Richards family. *PLOS ONE*, *12*(6), e0178691. https://doi.org/10.1371/journal.pone.0178691

Torres, K., Sierra, S., Poutou, R., Carrascal, A., & Mercado, M. (2005). PATOGENESIS DE *Listeria monocytogenes*, MICROORGANISMO ZOONOTICO EMERGENTE. *Revista MVZ Córdoba*, *10*(1), 511–543.

Ulloa Ibarra, J. T., Grijalva Diaz, F., Arrieta Vera, J., & Ortega Arcega, M. I. (2017). TRATAMIENTO DEL MODELO DE RICHARDS. *http://www.enip.com.mx/ActaImpresa6-Master-.html*. http://dspace.uan.mx:8080/xmlui/handle/123456789/1080

Ulloa Ibarra, J. T., & Rodriguez Carrillo, J. A. (2010). El modelo logístico: Una alternativa para el estudio del crecimiento poblacional de organismos. *http://www.veterinaria.org/revistas/redvet/n030310/031004.pdf*. http://dspace.uan.mx:8080/xmlui/handle/123456789/990

Wei, J., Wang, B., Chen, Y., Wang, Q., Ahmed, A. F., Zhang, Y., & Kang, W. (2022). The Immunomodulatory Effects of Active Ingredients From Nigella sativa in RAW264.7 Cells Through NF-κB/MAPK Signaling Pathways. *Frontiers in Nutrition*, *9*. https://www.frontiersin.org/articles/10.3389/fnut.2022.899797

Wiesmann, V., Franz, D., Held, C., Münzenmayer, C., Palmisano, R., & Wittenberg, T. (2015). Review of free software tools for image analysis of fluorescence cell micrographs. *Journal of Microscopy*, *257*(1), 39–53. https://doi.org/10.1111/jmi.12184

Zheng, H., Li, J., Luo, X., Li, C., Hu, L., Qiu, Q., Ding, J., Song, Y., & Deng, Y. (2019). Murine RAW264.7 cells as cellular drug delivery carriers for tumor therapy: A good idea? *Cancer Chemotherapy and Pharmacology*, *83*(2), 361–374. https://doi.org/10.1007/s00280-018-3735-0